

# Seasonal [particulate organic](#) carbon dynamics of the Kolyma River tributaries, Siberia

Kirsi H. Keskkitalo<sup>1,2\*</sup>, Lisa Bröder<sup>1,3</sup>, Tommaso Tesi<sup>4</sup>, Paul J. Mann<sup>2</sup>, Dirk J. Jong<sup>1</sup>, Sergio Bulte Garcia<sup>1</sup>, Anna Davydova<sup>5</sup>, Sergei Davydov<sup>5</sup>, Nikita Zimov<sup>5</sup>, Negar Haghypour<sup>3,6</sup>, Timothy I. Eglinton<sup>3</sup> and Jorien E. Vonk<sup>1\*</sup>

<sup>1</sup>Department of Earth Sciences, Vrije Universiteit Amsterdam, Amsterdam, The Netherlands

<sup>2</sup>Department of Geography and Environmental Sciences, Northumbria University, Newcastle Upon Tyne, UK

<sup>3</sup>Department of Earth Sciences, Swiss Federal Institute of Technology, Zürich, Switzerland

<sup>4</sup>National Research Council, Institute of Polar Sciences in Bologna, Italy

10 <sup>5</sup>Pacific Geographical Institute, Far East Branch, Russian Academy of Sciences, Northeast Science Station, Cherskiy, Republic of Sakha, Yakutia, Russia

<sup>6</sup>Laboratory of Ion Beam Physics, Swiss Federal Institute of Technology, Zürich, Switzerland

*Correspondence to:* Kirsi H. Keskkitalo (kirsi.keskkitalo@northumbria.ac.uk) and Jorien E. Vonk (j.e.vonk@vu.nl)

**Abstract.** Arctic warming is causing permafrost thaw and release of organic carbon (OC) to fluvial systems. Permafrost-derived OC can be transported downstream and degraded into greenhouse gases that may enhance climate warming. Susceptibility of OC to decomposition depends largely upon its source and composition which varies throughout the seasonally distinct hydrograph. Most studies [on carbon dynamics](#) to date have focused on larger Arctic rivers, yet little is known about carbon [cycling dynamics](#) in lower order rivers/streams. Here, we characterize composition and sources of OC, focusing on less studied particulate OC (POC), in smaller waterways within the Kolyma River watershed. Additionally, we examine how watershed characteristics control carbon concentrations. In lower order systems, we find rapid initiation of primary production in response to warm [water temperatures during spring freshet weather](#), shown by decreasing  $\delta^{13}\text{C}$ -POC, in contrast to larger rivers. [This results in CO<sub>2</sub> uptake by primary producers and microbial degradation of mainly autochthonous OC, however, if terrestrially derived inorganic carbon is assimilated by primary producers, also CO<sub>2</sub> emissions may occur.](#) As Arctic warming and hydrologic changes may increase OC transfer from smaller waterways ~~through to larger~~ river networks, [understanding carbon dynamics in smaller waterways is crucial. this may intensify inland water carbon outgassing.](#)

## 1 Introduction

The Arctic is warming up to four times the rate of the global average (Meredith et al., 2019; Rantanen et al., 2022) which affects hydrology, carbon cycling and permafrost (Turetsky et al., 2019; Walvoord and Kurylyk, 2016). Terrestrial permafrost thaw adds organic carbon (OC) to fluvial systems via active layer leaching and abrupt thaw processes (e.g., river bank erosion), the former releasing predominantly dissolved OC (DOC) and the latter particulate OC (POC) (Guo et al., 2007; Schuur et al.,

2015). Mineralization of terrestrially derived permafrost OC in fluvial systems adds greenhouse gases into the atmosphere enhancing climate warming (Meredith et al., 2019; Schuur et al., 2015).

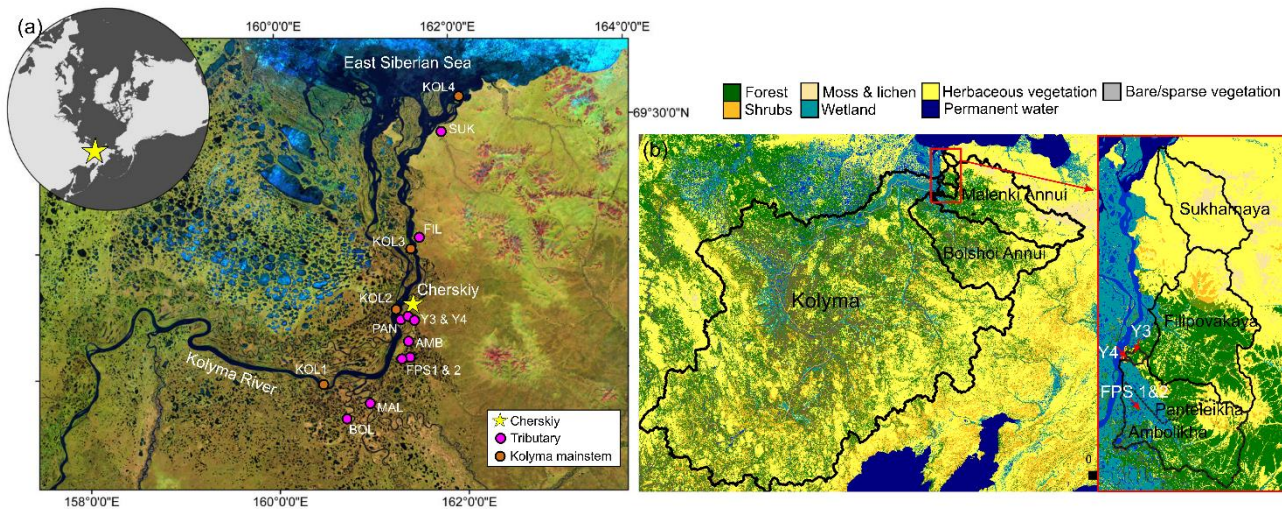
35 Mineralization dynamics of fluvial OC are largely determined by its composition. Modern-aged DOC predominantly fuels CO<sub>2</sub> emissions from Arctic waters (Dean et al., 2020), yet permafrost DOC is preferentially degraded when present (Mann et al., 2015; Vonk et al., 2013). The fluxes, composition, and degradation of mainstem-POC have been addressed in large Arctic rivers (e.g., Bröder et al., 2020; Guo and Macdonald, 2006; Keskitalo et al., 2022; McClelland et al., 2016), but our understanding of the carbon dynamics, especially regarding POC, and seasonality of smaller waterways are lacking.

40 Here, we investigate carbon characteristics (POC, DOC, dissolved inorganic carbon - DIC, stable carbon isotope  $\delta^{13}\text{C}$  of these carbon pools, and radiocarbon  $\Delta^{14}\text{C}$ -POC) and water chemistry (temperature, pH, conductivity, and water isotopes  $\delta^{18}\text{O}$  and  $\delta^2\text{H}$ ) in lower order streams/ivers within the Kolyma watershed (Fig. 1). We perform source-apportionment modelling to characterize sources of POC, and investigate how seasons and spatial characteristics (e.g., slope, soil OC content) affect carbon contributions in these streams. A future intensification of the Arctic hydrological cycle combined with longer growing season, earlier onset of spring freshet and on-going permafrost thaw is expected to shunt organic matter more rapidly from land into lower order streams/ivers and into large river systems. It is therefore necessary to understand carbon dynamics of lower order  
45 systems in order to project future changes within Arctic rivers (Collins et al., 2021; Mann et al., 2022; Raymond et al., 2016; Stadnyk et al., 2021).

## 2 Materials and Methods

### 2.1 Study area and background

50 The Kolyma River drains 100 % continuous permafrost terrain (Holmes et al., 2012) with variable landscapes including wetlands, tundra and forests (Mann et al., 2012). Here, permafrost consists partially of the OC- and ice-rich Yedoma sediments, which date to the Pleistocene (Strauss et al., 2017, 2021; Zimov et al., 2006). The continental climate encompasses cold winters (January mean -32.7 °C) and mild summers (July mean 13.2 °C) (Fedorov-Davydov et al., 2018b). River hydrology is characterized by a discharge peak ( $>30,000 \text{ m}^3 \text{ s}^{-1}$ ) during spring freshet (May–June), followed by a lower discharge (average of  $6,200 \pm 3000 \text{ m}^3 \text{ s}^{-1}$  in 2007–2017) during summer (July–August) (Shiklomanov et al., 2021). River OC concentrations  
55 follow the same pattern as discharge with higher concentrations during freshet than summer (Holmes et al., 2012; McClelland et al., 2016). All tributaries investigated in this study are partially underlain by Yedoma and located within the taiga or the tundra zone (Fig. 1) (Siewert et al., 2015; Strauss et al., 2021, 2022). Mean active layer thickness varies between catchments ranging from 154 cm in Panteleikha, 90 cm across the uplands (Y3), 65 cm at Ambolikha and 48 cm in tundra (measured at Cape Maliy Chukochiy) (Fedorov-Davydov et al., 2018a, 2018b).



60

**Figure 1.** (a) Sampling locations of the Kolyma River and tributaries (i.e., lower order streams). The tributaries are Sukharnaya (SUK), Filipovkaya (FIL), Panteleikha (PAN), Malenki Annui (MAL) and Bolshoi Annui (BOL). Ambolikha (AMB), Y3 and Y4 are tributaries of Panteleikha, and floodplain streams (FPS1 and FPS2) tributaries of Ambolikha. All the sites were sampled in both seasons: summer (July–August 2018) and freshet (June 2019). Map adapted from Mann et al. (2012) (b) Land cover of the Kolyma and its tributary watersheds. Land cover classes according to Buchhorn et al. (2020).

65

## 2.2 Field sampling

Surface water samples were collected in summer (July–August) 2018 and spring (June) 2019 (Fig. 1, Table A1) from ~20 cm depth from the middle of the tributary river/stream (one sample per river/stream per season, total n=10 tributaries per season) and additionally in the Kolyma mainstem (n=6 in spring and n=4 in summer) using pre-rinsed 1 L Nalgene bottles, which were decanted into a 10 L sterile and pre-rinsed polyethylene bag to maximize the sample size. During the spring freshet sampling campaign, all the rivers were ice-free during sampling. A few larger lakes in the area still had visible ice cover (5<sup>th</sup> of June 2019), but snow had largely melted and was only present in landscape depressions. The ice broke up in the Kolyma River mainstem 1<sup>st</sup> of June 2019 around the North East Science Station in Cherskiy. Water quality parameters were recorded using a multi-parameter sonde (Eijkelkamp Aquaread AP-800 in 2018, YSI Professional Plus in 2019).

70

75

Water samples were filtered (within 12 h) using pre-combusted (350 °C, 6 h) glass-fiber filters (Whatman, 0.7 µm). Prior to filtering, samples were vigorously agitated to ensure thorough particle mixing. Filters (POC samples) were frozen to -20 °C, while the filtrate (DOC samples, ~30 ml) was acidified with 30 µl of HCl (37 %) and stored cool (+5 °C). Samples for stable water isotopes ( $\delta^{18}\text{O}$ ,  $\delta^2\text{H}$ ) were filtered and stored cool (+5 °C) without headspace.

## 2.3 Analytical methods

### 80 2.3.1 Total suspended solids, organic carbon, and carbon isotope analyses

The amount of total suspended solids (TSS,  $\text{mg L}^{-1}$ ) was calculated by the difference in filter weight before and after filtering, divided by the volume of water filtered. For POC concentrations,  $\delta^{13}\text{C}$ -POC and total particulate nitrogen (TPN) filters were freeze-dried and subsampled by punching 18 % of the 45 mm filter area and fitted into silver capsules/boats. The subsamples were treated with 1M HCl to remove inorganic carbon, and then placed into an oven at 60 °C until dry. Afterwards, the samples were wrapped in tin capsules/boats to aid combustion during analysis. The samples were analyzed with a Thermo Fisher Elemental Analyzer (FLASH 2000 CHNS/O) coupled with a Thermo Finnigan Delta plus isotope ratio mass spectrometer (IRMS) at the National Research Council, Institute of Polar Sciences in Bologna, Italy.

For the  $^{14}\text{C}$  analysis, filters (see above for the subsampling method) were fumigated over 37 % HCl (72 h at 60 °C) to remove all inorganic carbon. After fumigation, samples were neutralized of excess acid (60 °C, a minimum of 48 h) in the presence of NaOH pellets, and subsequently wrapped in tin boats. The samples were analyzed using a coupled elemental analyzer-accelerator mass spectrometer (EA-AMS) system (vario MICRO cube, Elementar; Mini Carbon Dating System MICADAS, Ionplus, Dietikon, Switzerland) (Synal et al., 2007). The filter samples were blank corrected for constant contamination according to the method presented in Haghypour et al. (2019). The  $^{14}\text{C}$  analysis was carried out at the Laboratory of Ion Beam Physics at the Swiss Federal Institute of Technology (ETH), Zürich, Switzerland.

95 The DOC samples from summer 2018 were analyzed for OC and  $\delta^{13}\text{C}$ -DOC with an Aurora 1030 TOC analyzer (OI Analytical) coupled to a Delta V Advantage IRMS via a custom-built cryotrapping interface at KU Leuven, Belgium. Quantification and calibration were performed with IAEA-C6 ( $\delta^{13}\text{C} = -10.4 \text{ ‰}$ ) and an in-house sucrose standard ( $\delta^{13}\text{C} = -26.9 \text{ ‰}$ ) prepared in different concentrations. All  $\delta^{13}\text{C}$  data are reported in the notation relative to VPDB (Vienna Pee Dee Belemnite). The precision in duplicate samples was  $<5 \text{ ‰}$  for DOC, and  $0.2 \text{ ‰}$  for  $\delta^{13}\text{C}$ -DOC in  $>95 \text{ ‰}$  cases. The DOC samples from freshet 2019 were analyzed for OC and  $\delta^{13}\text{C}$ -DOC at the North Carolina State University, Raleigh, USA. For the method details, see Osburn and St-Jean (2007).

### 2.3.2 Dissolved inorganic carbon analyses

Samples for DIC were collected by filtering 4 ml of water into pre-evacuated 12 ml exetainer (Labco, UK) containing 100  $\mu\text{l}$  of  $\text{H}_3\text{PO}_4$  in 2018, while in 2019, DIC samples were filtered into exetainers containing 100  $\mu\text{L}$  of saturated KI and filled to the rim. The samples were stored cool ( $+5 \text{ °C}$ ) and dark until analysis. Headspace  $\text{CO}_2$  of the DIC samples from 2018 was analyzed using a Gasbench interfaced to a Thermo Delta V IRMS at the Northumbria University, UK. The DIC samples from 2019 were inserted into exetainers (pre-flushed with He) containing three drops of concentrated  $\text{H}_3\text{PO}_4$ . Subsequently, the  $\text{CO}_2$  was measured with a Finnigan GasBench II interfaced with a Thermo Finnigan Delta+ mass spectrometer at the Vrije Universiteit Amsterdam, The Netherlands. Analytical standard deviation for both instruments was  $<0.15 \text{ ‰}$ .

### 110 2.3.3 Analysis of water isotopes

We measured stable isotopes of oxygen and hydrogen ( $\delta^{18}\text{O}$ ,  $\delta^2\text{H}$ ) in water to characterize the hydrological conditions in the Kolyma River and its tributaries. Samples were analyzed with a Picarro Inc L2140-i Wavelength-scanning cavity ring-down spectrometer in replicates of seven, of which the first three were discarded to avoid carry-over effects. After a sequence of 10 samples, three in-house standards, all calibrated against international IAEA standards (VSLAP and VSMOW), were analyzed.

115 The fourth in-house standard (KONA) was used to control precision and accuracy of the measurements (standard deviation  $<0.1\text{‰}$  for  $\delta^{18}\text{O}$  and  $<2\text{‰}$  for  $\delta^2\text{H}$ ). The analysis was carried out at the Vrije Universiteit Amsterdam, The Netherlands.

### 2.4 Spatial analysis and landscape characterization

We delineated catchments using a 90 m digital elevation model (DEM) (Santoro and Strozzi, 2012) and determined mean soil OC content (SOCC) (Hugelius et al., 2013), land cover (Buchhorn et al., 2020) and calculated slope for each catchment using  
120 QGIS 3.16.1 with GRASS 7.8.4 (Fig. 1B). Prior to the spatial analysis, the DEM was pre-processed by filling all data gaps and sinks using algorithm described in Wang and Liu (2006). Two of the smallest catchments, FPS1 and FPS2, were delineated manually using a satellite image as a template, as the DEM resolution was too coarse for delineating these small and flat catchments. For the Kolyma River watershed, we used a delineation from Shiklomanov et al. (2021). Based on size and land cover, we grouped catchments into floodplain (FPS1, FPS2), headwater (Y3, Y4), tundra (Sukharnaya, Malenki Annu),  
125 wetland (Panteleikha, Ambolikha), and forest (Bolshoi Annu, Filipovkaya) stream/rivers and Kolyma mainstem as its own.

### 2.5 Source apportionment

For the source apportionment of POC, we used a Markov Chain Monte Carlo model to quantify contributions between autochthonous (i.e., primary production), active layer, terrestrial vegetation and permafrost sources. The source apportionment model accounts for uncertainties in the sources (i.e., endmembers), and estimates the residual error for the model (Stock and  
130 Semmens, 2016). We used a trophic discrimination factor (TDF) of zero assuming no discrimination (Stock and Semmens, 2016), and sampling year/season and river classes (e.g., tundra, headwater) as fixed effects for the model. The  $\delta^{13}\text{C}$  and  $\Delta^{14}\text{C}$  endmembers used were: autochthonous ( $\delta^{13}\text{C} -32.6 \pm 5.2\text{‰}$ ,  $n=157$ ;  $\Delta^{14}\text{C} -43.2 \pm 79\text{‰}$ ,  $n=79$ ), active layer ( $\delta^{13}\text{C} -26.4 \pm 0.8\text{‰}$ ,  $n=56$ ;  $\Delta^{14}\text{C} -198 \pm 148\text{‰}$ ,  $n=60$ ), terrestrial vegetation ( $\delta^{13}\text{C} -27.7 \pm 1.3\text{‰}$ ,  $n=94$ ;  $\Delta^{14}\text{C} 97 \pm 125\text{‰}$ ,  $n=58$ ) and permafrost ( $\delta^{13}\text{C} -26.3 \pm 0.7\text{‰}$ ,  $n=414$ ;  $\Delta^{14}\text{C} -777 \pm 106\text{‰}$ ,  $n=527$ ) according to Behnke et al. (2023), Levin et al. (2013), Vonk et al.  
135 (2012), Wild et al. (2019) and Winterfeld et al. (2015). See further details about the endmembers in [Appendix-Text A2](#).

For the model prior, we used a Dirichlet distribution as an uninformative (on the simplex) prior. We used the model with a chain length of 300,000, burn-in period of 200,000 and thinning of 100. The model was run in R (R Core Team, 2020) with a package *MixSiar* (Stock and Semmens, 2016). To evaluate the model convergence, we used the Gelman-Rubin and Geweke diagnostics, as well as the deviance information criteria. We report results as a mean  $\pm$  standard deviation.

## 140 2.6 Statistical analyses

We used linear regression to test how water temperature affects  $\delta^{13}\text{C}$ -POC, and how carbon isotopes depict POC-% to better understand river carbon dynamics. Additionally, we used linear regression to relate spatial catchment characteristics to organic carbon concentrations in rivers. For the linear regression model of water temperature and  $\delta^{13}\text{C}$ -POC;  $\delta^{13}\text{C}$ -POC and POC-%; and  $\Delta^{14}\text{C}$ -POC and POC-%, we used a function *lm*. The same function was used for linear regression of spatial parameters (slope and SOCC) and OC concentrations.

To test the difference in means in water chemistry parameters (water temperature, electrical conductivity — EC, pH and  $\delta^{18}\text{O}$ ) and carbon data (POC, DOC, DIC,  $\delta^{13}\text{C}$ -OC,  $\delta^{13}\text{C}$ -DIC and  $\Delta^{14}\text{C}$ -POC) between seasons (freshet vs summer) in the tributaries and the Kolyma mainstem, we used a Welch's- paired t-test. For the tributaries, n=10 for each season for each parameter (except n=8 for DIC and  $\delta^{13}\text{C}$ -DIC for summer), and for the Kolyma mainstem, n=6 during freshet and n=4 during summer for each parameter.

Additionally, we tested differences in above mentioned carbon parameters between differently sized streams/ rivers separately during freshet and summer using analysis of variance (ANOVA). We grouped the rivers in small (FPS1, FPS2, Y3, Y4), mid-sized (Panteleikha, Ambolikha, Sukharnaya, Filipovkaya) and large rivers (Malenki Annui, Bolshoi Annui, Kolyma mainstem). In the freshet, we analyzed small rivers n=4, mid-sized rivers n=4 and larger rivers n=6 for each parameter, and for summer, n=4 in small and mid-sized rivers and n=6 in large rivers (except for DIC and  $\delta^{13}\text{C}$ -DIC n=3 for small and mid-sized rivers and n=5 for large rivers). The significance level of all the statistical testing was 0.05. Testing was conducted in R (R Core Team, 2020). For further details on statistical methods, see Appendix Text A3.

~~For the linear regression model of water temperature and  $\delta^{13}\text{C}$ -POC;  $\delta^{13}\text{C}$ -POC and POC-%; and  $\Delta^{14}\text{C}$ -POC and POC-%, we used a function *lm*. The same function was used for linear regression of spatial parameters (slope and SOCC) and OC concentrations. The significance level of all the statistical testing was 0.05. Testing was conducted in R (R Core Team, 2020). For further details on statistical methods, see Appendix A.~~

## 3 Results

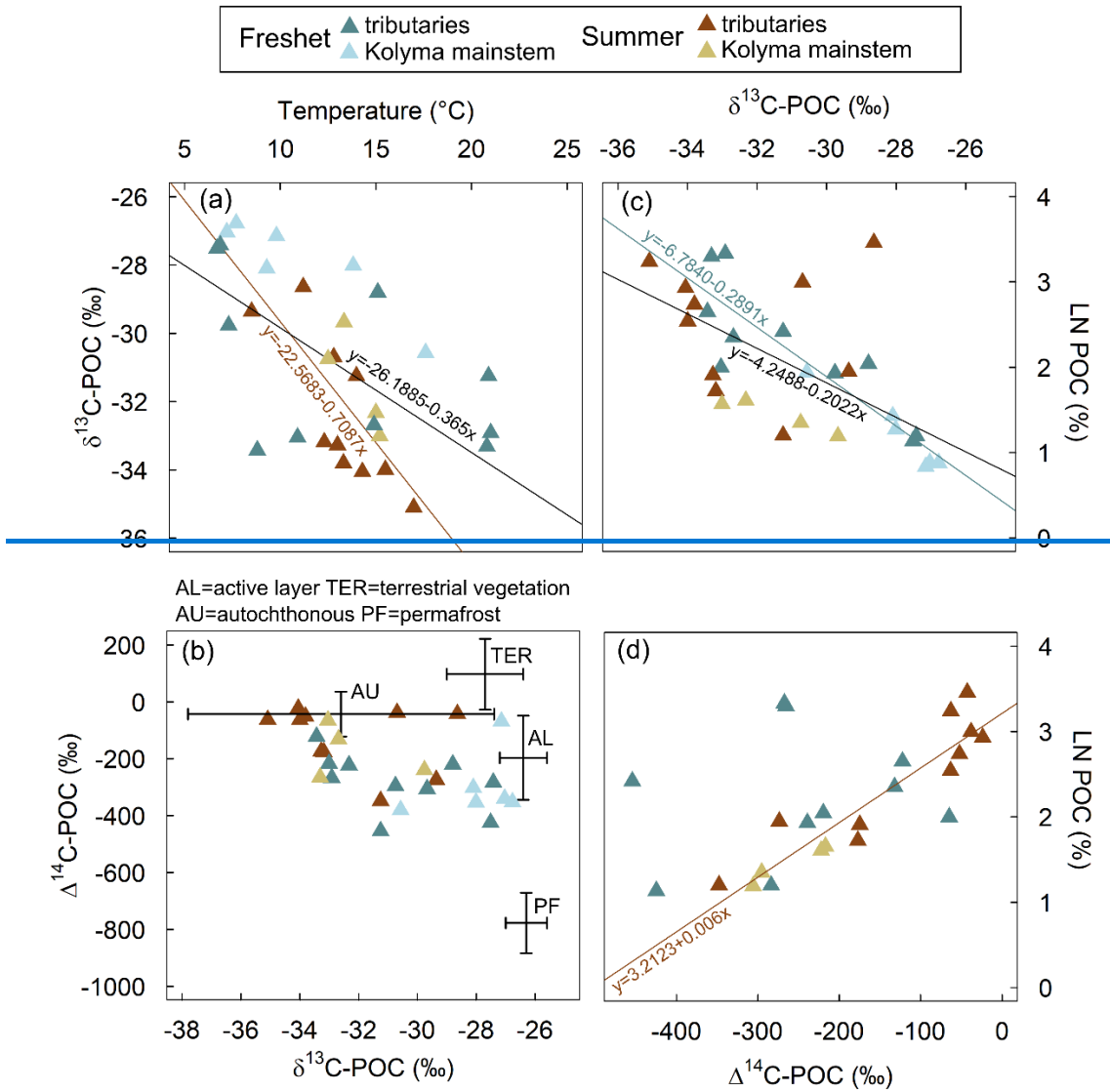
Part of the Kolyma River mainstem data that we present here has already been reported in Keskitalo et al. (2022), including water chemistry, OC concentrations, and isotopes for organic and inorganic carbon (Tables A1, A2, A3).

### 165 3.1 Catchment characteristics and water chemistry

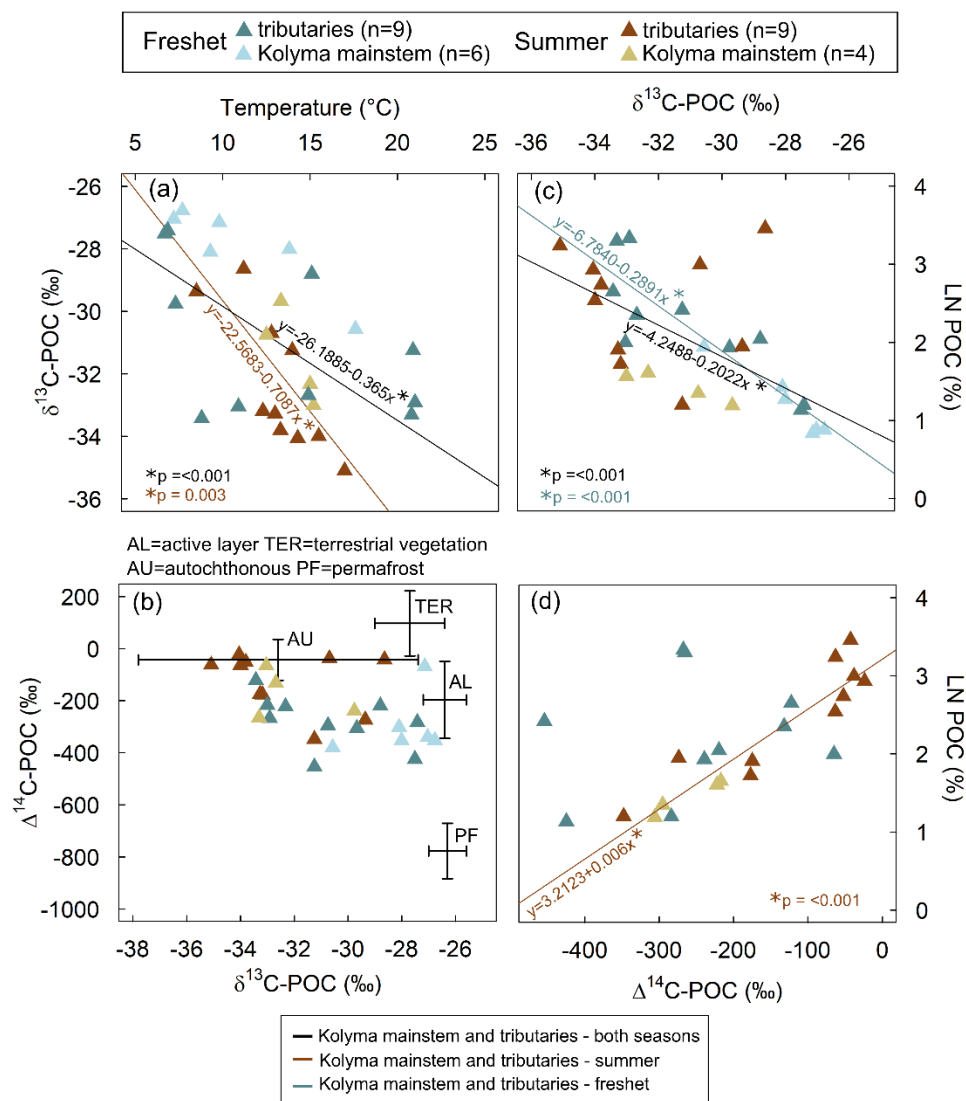
Tributary catchments ranged in size from  $<1 \text{ km}^2$  to nearly  $60,000 \text{ km}^2$  (Table A1). Mean SOCC varied between 269 and  $414 \text{ hg C/m}^2$  with the highest SOCC in the floodplain streams (FPS1, FPS2) and lowest in the tundra river Sukharnaya (Table A1). Mean catchment slope ranged from 0.01 to  $7^\circ$  with lowest slope in the floodplain streams and highest in the tundra river Malenki Annui (Table A1). Bolshoi Annui, Filipovkaya, Y3 and Y4 were largely covered by forest (55–74 %), while

170 Sukharnaya and Malenki Annuï showed highest coverage of herbaceous vegetation (53–84 %; Fig. 1B, Table A2). The floodplain streams had the highest fraction of wetland coverage (76–80 %).

Surface water temperatures did not significantly differ between freshet and summer in the tributaries ( $p=0.946$ ) or in the Kolyma mainstem ( $p=0.126167$ ), but showed a larger spatial variability during freshet (6.7 to 21 °C in tributaries; 7.2 and 18.0 °C in mainstem) ~~than in~~ compared to -summer (8.5 to 17 °C in tributaries; 12.5 to 15.0 °C in mainstem, Fig. 2A, Table 175 A6). The EC and water isotope ( $\delta^{18}\text{O}$ ) signature were lower during freshet than summer both in the tributaries ( $p<0.001$  and  $p<0.001$ , respectively) and the Kolyma mainstem ( $p<0.005001$  and  $p=0.048006$ , respectively; Tables 1, A2 and A6).







180 **Figure 2.** (a) Surface water temperature and  $\delta^{13}\text{C}$  of particulate organic carbon (POC). The linear regression for tributaries and Kolyma mainstem during both freshet and summer ( $R^2=0.33$ ,  $F(1,28)=15.07$ ,  $p<0.001$ ; black line) and only during summer ( $R^2=0.49$ ,  $F(1,12)=13.58$ ,  $p=0.003$ ; brown line) was statistically significant- while for freshet, or Kolyma mainstem and the tributaries separately, it was not (not shown). (b) The  $\Delta^{14}\text{C-POC}$  and  $\delta^{13}\text{C-POC}$ . Endmembers are indicated with arrows: OC from active layer (AL), terrestrial vegetation (TER), autochthonous (AU) and permafrost (PF) sources. Endmembers are according to Behnke et al. (2023), Levin et al. (2013), Vonk et al. (2012), Wild et al. (2019) and Winterfeld et al. (2015). See [appendix-Appendix A](#) for more details about endmembers. (c) The  $\delta^{13}\text{C-POC}$  and natural logarithm (LN) of POC-% (amount of POC of total suspended solids). The linear regression for the Kolyma mainstem and tributaries (both freshet and summer,  $R^2=0.39$ ,  $F(1,28)=19.36$ ,  $p<0.001$ ; black line) and separately for freshet was statistically significant ( $R^2=0.82$ ,  $F(1,14)=67.57$ ,  $p<0.001$ ; blue line). Linear regression for summer only was not significant, or for tributaries and Kolyma mainstem separately (not shown). (d) The  $\Delta^{14}\text{C-POC}$  as a function of LN POC-%. Linear regression for summer (both Kolyma mainstem and tributaries) was significant ( $R^2=0.85$ ,  $F(1,12)=75.4$ ,  $p<0.001$ ; brown line). Linear regression for the Kolyma mainstem or tributaries separately was not significant (not shown). All panels include data from freshet (June 2019) and summer (July–Aug 2018) in the Kolyma River mainstem and its tributaries. Part of the Kolyma data has been previously reported in Keskitalo et al. (2022).

185  
 190

## 3.2 Total suspended solids, carbon concentrations and isotopes of carbon

### 3.2.1 Seasonal carbon patterns across the catchment

195 Concentrations of TSS were higher during freshet than summer at most all sites, ~~(not statistically significant p=0.289; Tables 1, A6)~~ except at FPS1, FPS2 and Y3, but was not statistically significant (p=0.1309; Tables 1, A6) that showed the opposite pattern. Concentrations of POC and TPN largely followed the same trend (not statistically significant, p=0.457–391 and p=0.669599, respectively; Table A6). In the Kolyma mainstem, POC concentrations were higher during freshet than summer (p=0.049; Table A6), while TSS and TPN showed a similar pattern (not statistically significant, p=0.071–09 and p=0.09306, respectively). In the tributaries, DOC concentrations did not differ between seasons (p=0.242153), while DIC concentrations were lower during freshet than summer (p=<0.005003; Table A6). In the Kolyma mainstem, DOC concentrations were higher during freshet than summer (p=<0.005001) while DIC showed the opposite pattern (not statistically significant p=0.01508; Table A6). Of the total carbon pool (POC, DOC and DIC), POC was the smallest carbon fraction both during freshet and summer (Fig. 3, Table A7).

205 In the tributaries, the  $\delta^{13}\text{C}$ -POC did not differ between seasons (p=0.320281) while  $\delta^{13}\text{C}$ -DOC were higher during freshet than in summer (p=<0.001; Table A6). In the Kolyma mainstem, both  $\delta^{13}\text{C}$ -POC (not statistically significant p=0.045) and  $\delta^{13}\text{C}$ -DOC (p=0.0052; Table A6) showed higher values during freshet than summer. The  $\Delta^{14}\text{C}$ -POC were lower (i.e., older) during freshet than summer in the tributaries (p=0.0296) while in the Kolyma mainstem the trend was similar, but not statistically significant (p=0.945; Fig. 2B, Table A6). While we did not measure  $\Delta^{14}\text{C}$ -DOC, we report previously unpublished data (May–October 2006–2011) at FPS, Y3, Y4 and Pantheleikha (Table A10) showing that all DOC is modern. The  $\delta^{13}\text{C}$ -DIC was lower during freshet than summer both in the tributaries (p=<0.001) and in the Kolyma mainstem (p=0.0042; Table A6).

### 3.2.2 Carbon patterns between different sized rivers during freshet and summer

215 During freshet, large rivers showed higher TSS, POC and lower DOC concentrations than small ones (p=0.0017, p=0.048 and p=0.018029, respectively), while POC, TPN and DIC did not differ between different sized rivers (Table A8). The POC-% (amount of OC of TSS) was higher in small and mid-sized rivers than large ones during freshet (p=0.03405 and 0.016, respectively) and summer (p=0.0162 and 0.048, respectively; Fig. 4, Table A8). In summer, DOC concentrations were higher in small rivers than in large ones (p=0.02903) while TSS and POC were lower (p=0.001 and 0.048, respectively); TPN and DIC did not differ between different sized rivers during summer (Table A8).

220 ~~In the tributaries, the  $\delta^{13}\text{C}$ -POC did not differ between seasons (p=0.320) while  $\delta^{13}\text{C}$ -DOC were higher during freshet than in summer (p=<0.001; Table A6). In the Kolyma mainstem, both  $\delta^{13}\text{C}$ -POC (p=0.01) and  $\delta^{13}\text{C}$ -DOC (p=0.005; Table A6) showed higher values during freshet than summer. The  $\Delta^{14}\text{C}$ -POC were lower (i.e., older) during freshet than summer in the~~

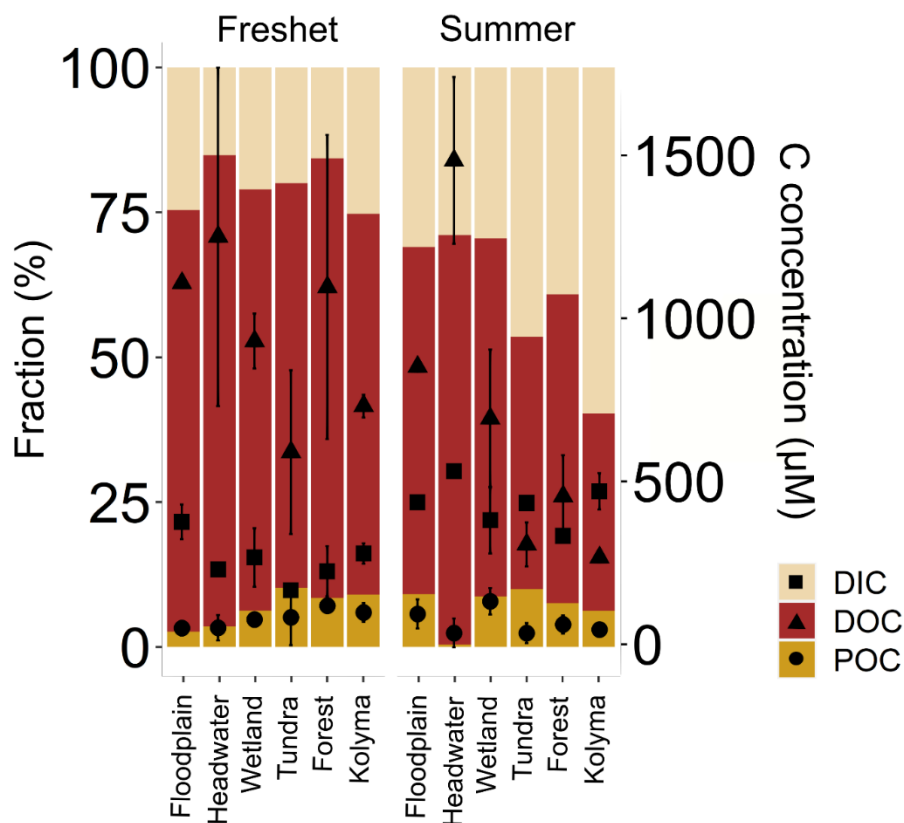
225 ~~tributaries ( $p=0.029$ ) while in the Kolyma mainstem the trend was similar, but not statistically significant ( $p=0.94$ ; Fig. 2B, Table A6). While we did not measure  $\Delta^{14}\text{C-DOC}$ , we report previously unpublished data (May–October 2006–2011) at FPS, Y3, Y4 and Pantheleikha (Table A10) showing that all DOC is modern. The  $\delta^{13}\text{C-DIC}$  was lower during freshet than summer both in the tributaries ( $p<0.001$ ) and in the Kolyma mainstem ( $p=0.004$ ; Table A6).~~

230 During freshet, small and midsized rivers showed lower  $\delta^{13}\text{C-POC}$  than large rivers ( $p=0.039$ ) while only midsized rivers showed also lower  $\delta^{13}\text{C-DOC}$  ( $p=0.026$ ; Table A8). During summer, the  $\Delta^{14}\text{C-POC}$  was higher (i.e., younger) in the small and midsized rivers than in the large ones (only significant for the small ones  $p=0.044$ ; Fig. 4). In summer, there was no significant difference in  $\delta^{13}\text{C-OC}$  and  $\delta^{13}\text{C-DIC}$  between differently sized rivers (Table A8).

**Table 1.** Concentrations of total suspended solids (TSS), particulate and dissolved organic carbon (POC and DOC, respectively), dissolved inorganic carbon (DIC) in the tributary streams and the Kolyma River during freshet (June 2019) and summer (July–Aug 2018). Watershed types (WST) are abbreviated as headwaters (H), floodplain (FP), wetland (W), tundra (T) and forest (F). Tributary streams are abbreviated as AMB=Ambolikha, SUK=Sukhamaya, PAN=Panteleikha, FIL=Filipovkaya, MAL=Malenki Annui and BOL=Bolshoi Annui. The Kolyma mainstem is abbreviated as KOL. Also shown are stable and radioisotopes of carbon:  $\delta^{13}\text{C}$  of POC, DOC and DIC, and  $\Delta^{14}\text{C}$ -POC, and concentrations of total particulate nitrogen (TPN), molar ratio of POC/TPN and water isotopes ( $\delta^{18}\text{O}$ ;  $\delta\text{H}$ ). For DIC,  $\delta^{13}\text{C}$ -DIC,  $\Delta^{14}\text{C}$ -POC and water isotopes, mean  $\pm$  analytical standard deviation is shown. For the Kolyma River, mean  $\pm$  standard deviation between different sampling locations (freshet n=6, summer n=4) is indicated, including standard deviation between replicate samples (Table A2) and analytical uncertainties when applicable. Additionally, we show mean (Average)  $\pm$  standard deviation of all tributaries. Further information regarding the watersheds (e.g., size, land cover) is available in Appendix A.

River	WST	TSS (mg/L)	POC ( $\mu\text{M}$ )	POC (%)	$\delta^{13}\text{C}$ -POC (%)	$\Delta^{14}\text{C}$ -POC (%)	TPN ( $\mu\text{M}$ )	POC/TPN	DOC ( $\mu\text{M}$ )	$\delta^{13}\text{C}$ -DOC (%)	DIC ( $\mu\text{M}$ )	$\delta^{13}\text{C}$ -DIC (%)	$\delta^{18}\text{O}$ (‰)
Y4	H	7.0	82.1	14	-33.43	-122 $\pm$ 21	8.31	8.5	887	-26.86	220 $\pm$ 9	-16.02 $\pm$ 0.1	-22.81 $\pm$ 0.1
Y3	H	4.7	26.8	6.9	-29.76	-239 $\pm$ 24	2.34	8.7	1621	-27.22	246 $\pm$ 5	-15.72 $\pm$ 0.2	-22.58 $\pm$ 0.4
FPS1	FP	4.4	40.7	11	-31.25	-454 $\pm$ 26	2.80	12.5	1110	-28.56	376 $\pm$ 16	-17.67 $\pm$ 0.3	-23.30 $\pm$ 0.0
FPS2	FP	2.8	65.9	28	-32.92	-268 $\pm$ 29	5.51	10.2	1115	-26.50	384 $\pm$ 11	-15.32 $\pm$ 0.2	-23.04 $\pm$ 0.2
AMB	W	9.5	85.4	11	-32.68	-132 $\pm$ 26	10.8	6.6	994	-29.06	334 $\pm$ 9	-18.45 $\pm$ 0.2	-22.75 $\pm$ 0.0
SUK	T	4.0	25.9	7.7	-28.80	-220 $\pm$ 21	2.73	8.1	416	-27.34	161 $\pm$ 2	-10.91 $\pm$ 0.1	-22.34 $\pm$ 0.1
PAN	W	13	77.6	7.4	-33.04	-65.1 $\pm$ 26	8.04	8.3	874	-26.86	207 $\pm$ 8	-15.93 $\pm$ 0.5	-22.64 $\pm$ 0.1
FIL	F	4.8	107	27	-33.31	-265 $\pm$ 25	11.2	8.2	1430	-28.47	282 $\pm$ 11	-12.54 $\pm$ 0.0	-22.56 $\pm$ 0.1
MAL	T	54	148	3.3	-27.42	-284 $\pm$ 27	15.7	8.1	771	-26.21	178 $\pm$ 22	-17.05 $\pm$ 0.4	-22.70 $\pm$ 0.2
BOL	F	53	138	3.1	-27.51	-425 $\pm$ 299	12.6	9.4	770	-26.44	174 $\pm$ 4	-16.66 $\pm$ 0.1	-22.88 $\pm$ 0.1
Average	-	16 $\pm$ 20	79.5 $\pm$ 42	12 $\pm$ 8.9	-31.01 $\pm$ 2.4	-247 $\pm$ 158	8.0 $\pm$ 4.6	8.9 $\pm$ 1.6	999 $\pm$ 345	-27.35 $\pm$ 1.0	256 $\pm$ 91	-15.63 $\pm$ 2.4	-22.58 $\pm$ 4
KOL	-	39 $\pm$ 26	91.6 $\pm$ 36	3.6 $\pm$ 1.9	-27.94 $\pm$ 1.4	-299 $\pm$ 71	8.2 $\pm$ 2.9	9.4 $\pm$ 0.9	708 $\pm$ 75	-26.70 $\pm$ 0.4	283 $\pm$ 85	-13.09 $\pm$ 1.6	-22.52 $\pm$ 2
Y4	H	0.3	7.8	32	-28.64	-42.7 $\pm$ 27	0.60	11.2	1308	-29.51	535 $\pm$ 0.3	-15.27 $\pm$ 0.1	-18.61 $\pm$ 0.1
Y3	H	15	70.5	5.6	-30.65*	-177 $\pm$ 20	4.96	12.2	1670	-29.20	n/a	n/a	-20.09 $\pm$ 0.1
FPS1	FP	7.8	129	20	-30.70	-38.2 $\pm$ 18	7.15	15.5	846	-29.46	438 $\pm$ 0.2	-12.10 $\pm$ 0.0	-21.39 $\pm$ 0.1
FPS2	FP	5.1	66.2	15	-33.80	-52.3 $\pm$ 18	5.77	9.8	865	-29.72	442 $\pm$ 0.2	-8.31	-20.07 $\pm$ 0.0
AMB	W	8.1	85.8	13	-34.00	-63.2 $\pm$ 17	9.42	7.8	806	-29.38	457 $\pm$ 0.2	-12.38 $\pm$ 0.0	-21.15 $\pm$ 0.1
SUK	T	2.9	16.7	7.0	-29.36	-274 $\pm$ 24	1.44	9.9	359	-28.77	n/a	n/a	-18.97 $\pm$ 0.0
PAN	W	9.2	143	19	-34.06	-23.9 $\pm$ 18	19.0	6.5	809	-31.16	313 $\pm$ 0.1	-11.42 $\pm$ 0.1	-20.95 $\pm$ 0.0
FIL	F	4.0	84.5	25	-35.10	-62.9 $\pm$ 17	10.9	6.7	548	-29.65	328 $\pm$ 0.1	-8.02 $\pm$ 0.0	-20.48 $\pm$ 0.0
MAL	T	22	60.0	3.3	-31.25	-348 $\pm$ 18	6.29	8.2	263	-28.91	281 $\pm$ 0.1	-9.91 $\pm$ 0.1	-20.20 $\pm$ 0.1
BOL	F	8.1	45.4	6.7	-33.27	-175 $\pm$ 19	5.31	7.3	368	-29.47	346 $\pm$ 0.1	-10.60 $\pm$ 0.1	-21.01 $\pm$ 0.0
Average	-	8.2 $\pm$ 6	70.9 $\pm$ 43	15 $\pm$ 9.4	-32.08 $\pm$ 2.2	-126 $\pm$ 129	7.1 $\pm$ 5.2	9.5 $\pm$ 2.8	784 $\pm$ 441	-29.52 $\pm$ 0.7	393 $\pm$ 88	-11.0 $\pm$ 2.4	-20.29 $\pm$ 0.9
KOL	-	15 $\pm$ 7	51.7 $\pm$ 13	4.2 $\pm$ 0.9	-31.44 $\pm$ 1.5	-273 $\pm$ 77	5.9 $\pm$ 1.1	7.6 $\pm$ 0.9	271 $\pm$ 26	-29.24 $\pm$ 0.8	473 $\pm$ 56	-9.30 $\pm$ 0.2	-21.78 $\pm$ 0.4

240 \*average of a tributary of Y3 and Y3 mainstem upstream of the sampling site in 2018 as  $\delta^{13}\text{C}$  analysis at the sampling location was not successful.



243 **Figure 3.** Fractions (%) of different carbon pools: particulate and dissolved organic carbon (POC and DOC, respectively) and  
 244 dissolved inorganic carbon (DIC) in the Kolyma River and its tributary rivers/streams during freshet (2019) and summer (2018).  
 245 On the right-side y-axis, concentrations of respective carbon pools are shown with square (DIC), triangle (DOC) and circle  
 246 (POC) symbols with mean  $\pm$  standard deviation between samples. The tributaries are grouped based on their land cover and  
 247 size as follows (n=2 per group per season except for the Kolyma mainstem n=6 during freshet and n=4 during summer): tundra  
 248 = Sukharnaya and Malenki Annui; headwater (small, forested watersheds) = Y3, Y4; floodplain = FPS1 and FPS2; wetland  
 249 (influenced) = Ambolikha and Panteleikha; forest (larger forested watersheds) = Filipovkaya and Bolshoi Annui; Kolyma =  
 250 Kolyma mainstem. The DIC concentrations were not measured for Sukharnaya and Y3 during summer.

### 252 3.3 Source apportionment

253 Both during freshet and summer, POC was largely autochthonous in the tributaries (34–82 % and 56–92 %,  
254 respectively; Fig. 5, Table A11) and in the Kolyma mainstem (35 and 59 %, respectively). Permafrost-derived  
255 POC was higher during freshet than summer at all sites (tributaries 8–33 % during freshet and 3–22 % during  
256 summer; mainstem 34 % during freshet and 22 % during summer). Contributions from active layer and terrestrial  
257 vegetation were lowest to tributary-POC (8–24 % and 4–10% during freshet, respectively; 3–16 % and 2–7 %  
258 during summer, respectively; Fig. 5). Similarly, active layer and terrestrial vegetation contributed least to the  
259 Kolyma-~~POC waters~~ during freshet (9–22 %) and summer (6–13 %; Table A11).

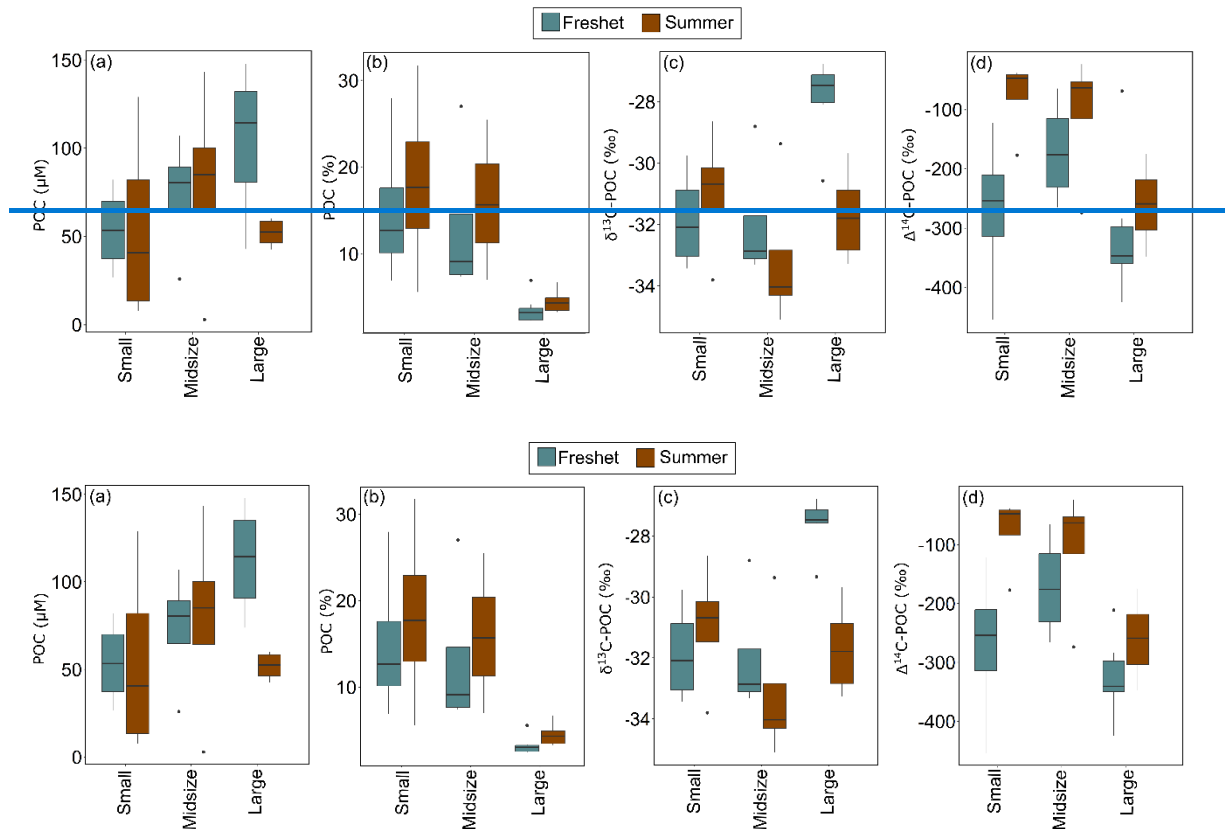
## 260 4 Discussion

261 [Our results show contrasting water chemistry and carbon dynamics between spring freshet and summer in the](#)  
262 [Kolyma River tributaries and mainstem, while POC pool is mostly autochthonous both in the tributaries and the](#)  
263 [Kolyma mainstem during both seasons. Small and mid-sized rivers differ in their POC composition from large](#)  
264 [rivers with higher POC-% \(freshet and summer\), lower  \$\delta^{13}\text{C}\$ -POC \(freshet\) and higher  \$\Delta^{14}\text{C}\$  \(summer\).](#)

### 265 4.1 Smaller tributary streams may start primary production earlier than larger rivers in the spring

266 In all tributaries and the Kolyma mainstem, the water isotope  $\delta^{18}\text{O}$  signature significantly differed between seasons  
267 (Table A6). Lower  $\delta^{18}\text{O}$  signal during freshet suggests that snowmelt was the dominant water source (Welp et al.,  
268 2005), supported by lower EC values (Table A6). However, water temperatures varied more within a season than  
269 between seasons both in the tributaries and in the Kolyma (Table A6). Air temperatures were particularly warm  
270 during freshet 2019 (see Fig. A2 for average air temperatures in 2007–2017) that was reflected as warm water  
271 temperatures especially in Filipovkaya and the floodplain streams (>20 °C). These high temperatures likely  
272 promoted a rapid onset of autochthonous production as suggested by relatively low  $\delta^{13}\text{C}$ -POC (up to -33.43 ‰)  
273 for the season, combined with high POC-% (11–28 %, Fig. 2C). However, in tributaries Y4, Panteleikha and  
274 Ambolikha low  $\delta^{13}\text{C}$ -POC occurred already prior to the high air temperatures (Table A3), suggesting that other  
275 factors such as higher nutrient fluxes during freshet likely also play a role in inducing primary production (Harrison  
276 and Cota, 1991; Holmes et al., 2012; Mann et al., 2012). [While the POC pool is dominated by autochthonous OC,](#)  
277 [it is likely that allochthonous OC is also present, as suggested by POC/TPN ratios \(e.g., Meyers, 1994\) and our](#)  
278 [source apportionment results \(see Section 4.3 and Fig. 5\).](#) Water temperature explained 33 % of the variability in  
279  $\delta^{13}\text{C}$ -POC overall (higher temperature indicating lower  $\delta^{13}\text{C}$ -POC), while during summer it explained ~50 % of  
280 its variability (Fig. 2A), confirming that other factors affect  $\delta^{13}\text{C}$ -POC. Overall, freshet  $\delta^{13}\text{C}$ -POC was lower and  
281 POC-% higher in small and mid-sized rivers compared to the large ones (Fig. 4; Table A8), suggesting that river  
282 size may play a role in the timing for primary production onset during freshet. Higher input of (terrestrial) DOC  
283 (via degradation to inorganic carbon to be taken up by primary producers) and/or nutrients combined with shorter  
284 transport times may enhance primary production in smaller streams during freshet. In contrast, large rivers have  
285 longer transport times, and nutrients may already have been utilized (in headwaters), and terrestrially derived DOC  
286 degraded (Denfeld et al., 2013). Our POC data suggest that autochthonous production may start sooner in small  
287 and mid-sized tributaries than in large rivers during freshet.

288



289

290

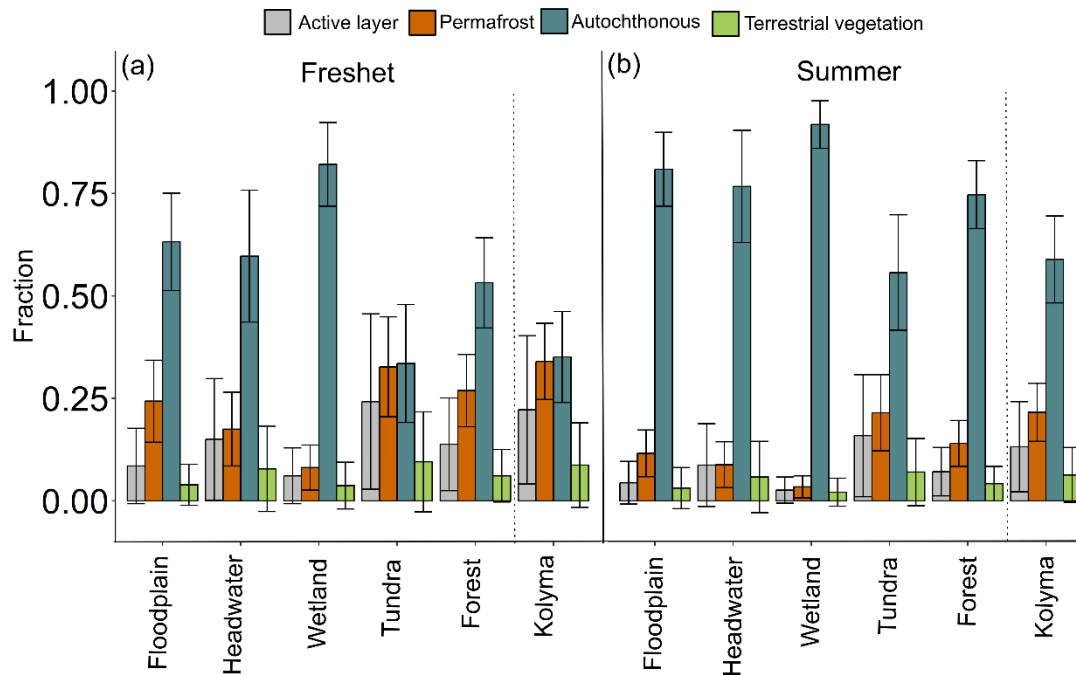
291 **Figure 4.** Concentrations of particulate organic carbon (POC) in (a)  $\mu\text{M}$  (no statistically significant differences between  
 292 different size groups) and (b) in percent POC in small, midsize, and large rivers during freshet and summer (small and  
 293 midsize rivers were significantly different from the large rivers both during summer and freshet). The (c)  $\delta^{13}\text{C}$ -POC (small  
 294 and midsize rivers were significantly different from large rivers during freshet) and (d)  $\Delta^{14}\text{C}$ -POC in small, midsize, and  
 295 large rivers during freshet and summer (small rivers were significantly different from large ones during summer). Boxplots  
 296 show median (line), interquartile range (the box) and minimum and maximum (whiskers). For small rivers  $n=4$  per season,  
 297 for midsize rivers  $n=4$  per season and for large rivers  $n=6$  per season in summer and  $n=9$  in freshet. See Table A8 for analysis of  
 298 variance (ANOVA) results regarding statistically significant differences between different sized rivers.

299 **4.2 Organic and inorganic carbon dynamics differ between the tributaries and the Kolyma River mainstem**

300 **4.2.1 Suspended matter dynamics**

301 During freshet, mean TSS and POC concentrations were higher in the large rivers than in the small tributary rivers  
 302 (statistically significant only for TSS; Table A8) likely due to higher river power causing greater bank erosion  
 303 (delivering sediment and POC) as well as higher turbulence promoting particle suspension (Striegl et al., 2007).  
 304 Spatial characteristics such as catchment slope or SOCC did not show a linear relationship with summer-POC,  
 305 indicating that other factors, such as abrupt permafrost thaw, primary production, and water temperature, likely  
 306 play a more important role in driving POC concentrations (Fig. A3, Sect. 4.3). In the Kolyma, POC and  $\delta^{13}\text{C}$ -POC  
 307 were significantly different between seasons (significant only for POC), while in the tributaries there was  
 308 no significant difference (Table A6). This likely suggests both local variability and stronger fluctuations in the  
 309 tributaries that react faster to environmental changes such as high air temperatures.

310



311  
 312 **Figure 5.** Fractions of different particulate organic carbon (POC) sources (active layer, terrestrial vegetation, autochthonous  
 313 and permafrost) according to Markov Chain Monte Carlo source apportionment modelling using  $\delta^{13}\text{C}$  and  $\Delta^{14}\text{C}$  during (a)  
 314 freshet and (b) summer. The dashed lines separate the Kolyma mainstem from the tributaries. For each catchment type  
 315 (floodplain, headwater, wetland, tundra and forest)  $n=2$  for the number of tributaries per season while for the Kolyma mainstem  
 316  $n=6$  during freshet and  $n=4$  during summer. The endmembers were according to Behnke et al. (2023), Levin et al. (2013), Vonk  
 317 et al. (2012), Wild et al. (2019) and Winterfeld et al. (2015), see more information in the Appendix A.

#### 318 4.2.2 Dissolved matter dynamics

319 Previous studies have shown that lower order streams differ from the Kolyma River in their dissolved carbon  
 320 concentrations and composition (Drake et al., 2018a; Mann et al., 2012; Rogers et al., 2021). Similarly, our results  
 321 show that DOC concentrations were higher in the small tributaries than in the large ones both during freshet and  
 322 summer, while  $\delta^{13}\text{C}$ -DOC differed only between midsized and large rivers during freshet (lower for midsized  
 323 rivers; Table A8). In the tributaries, SOCC predicted nearly half of the variability in DOC concentrations during  
 324 summer (Fig. A3). It has been shown that the majority of DOC in the Kolyma mainstem originates from modern  
 325 vegetation rather than permafrost sources (Rogers et al., 2021), potentially due to rapid degradation of permafrost-  
 326 derived DOC during transit from the headwaters (Mann et al., 2015). Similarly, the  $\Delta^{14}\text{C}$ -DOC shows a modern  
 327 signal for FPS, Y4, Y3 and Panteleikha (Table A10), implying that small and midsized stream DOC is also  
 328 predominantly modern.

329 Both in the Kolyma mainstem and the tributaries, DIC and  $\delta^{13}\text{C}$ -DIC differed significantly between  
 330 seasons (Table A6) and followed a previously-reported trend in fluvial systems of lower concentrations and  $\delta^{13}\text{C}$ -  
 331 DIC during freshet than summer (Campeau et al., 2017; Waldron et al., 2007). In the Kolyma, only  $\delta^{13}\text{C}$ -DIC was  
 332 significantly lower during freshet than summer. Our Kolyma DIC concentrations were close to a previously  
 333 reported concentration (Drake et al., 2018b), while  $\delta^{13}\text{C}$ -DIC values were  $\sim 2\text{‰}$  higher in our study. The higher  
 334 DIC concentrations during summer may reflect an increase in leaching from the active layer and/or re-  
 335 mineralization of DOC, while the higher  $\delta^{13}\text{C}$ -DIC suggests primary production and/or partial  $\text{CO}_2$  evasion, where  
 336 part of the  $\text{CO}_2$  is likely sourced from degraded permafrost (Campeau et al., 2017; Drake et al., 2018b; Powers et



337 al., 2017; Waldron et al., 2007). During freshet, DIC concentrations were higher in watersheds with higher water  
338 temperatures, a trend not observed during summer (Table 1, [Table A3](#)). While higher temperatures may increase  
339 CO<sub>2</sub> evasion and thus lower DIC concentrations (and increase δ<sup>13</sup>C-DIC) (Campeau et al., 2017), on-going OC  
340 degradation [and/or leaching of terrestrially derived DIC](#) potentially keeps the concentrations high. The higher δ<sup>13</sup>C-  
341 DIC of the Kolyma mainstem, Sukharnaya and Filipovkaya, suggests that they may be affected by CO<sub>2</sub> evasion  
342 during turbulent freshet conditions. At Filipovkaya, these high ratios may be partially due to primary production  
343 (i.e., biological consumption of DIC) as the δ<sup>13</sup>C-POC is relatively low (Table 1). In headwater streams,  
344 contribution of OC mineralization to the DIC pool has been suggested to be negligible relative to terrestrial input  
345 (Winterdahl et al., 2016). Smaller streams have been shown to evade more CO<sub>2</sub> to the atmosphere than larger rivers  
346 during summer, thus suggesting that CO<sub>2</sub> evasion from smaller streams is mainly driven by hydrological flow  
347 paths and terrestrial OC, while in the larger rivers autochthonous production dominates as a CO<sub>2</sub> sink (Denfeld et  
348 al., 2013). Finally, weathering, dominated by carbonates and silicates in the Kolyma watershed, may add to the  
349 DIC concentrations (Tank et al., 2012).

### 350 **4.3 The importance of autochthonous production: riverine POC dominates in the tributaries**

351 Tributary-POC is mostly autochthonous both during freshet (58 ± 33 %) and summer (76 ± 27 %) indicating high  
352 primary production, especially in summer (Fig. 5), supported by higher OC-% in small and mid-sized tributaries  
353 (6.9–20 % and 5.6–32 %, respectively) than in the large rivers (~3 % and 3–7 %, respectively; Tables A8). The  
354 Δ<sup>14</sup>C-POC was significantly higher (i.e., younger) in tributaries during summer than freshet, likely due to higher  
355 primary production, while in the Kolyma Δ<sup>14</sup>C-POC did not significantly differ between seasons as shown  
356 previously (Bröder et al., 2020; McClelland et al., 2016). Filipovkaya and the floodplain streams (FPS1, FPS2)  
357 showed relatively low Δ<sup>14</sup>C-POC combined with high POC-% and low δ<sup>13</sup>C-POC (Fig. 2C–D), suggesting  
358 incorporation of old CO<sub>2</sub> into biomass, likely originating from rapid degradation of permafrost-derived DOC  
359 (Drake et al., 2018b). The permafrost fraction was relatively low during summer due to dominance of primary  
360 production (Behnke et al., 2023), which was particularly pronounced in the smaller waterways (Fig. 5).

361 In an earlier incubation study, we showed that riverine-produced POC (with low δ<sup>13</sup>C-POC) in Kolyma  
362 summer waters degrades rapidly (degradation constant k=-0.026 day<sup>-1</sup>), while terrestrially-produced POC in  
363 freshet waters did not show OC loss (Keskitalo et al., 2022). Furthermore, we showed that a lower initial δ<sup>13</sup>C-  
364 POC corresponded to a higher POC loss. Therefore, the low δ<sup>13</sup>C-POC of small and mid-sized streams during  
365 freshet suggests that POC may be prone to degradation, while POC degradation in the Kolyma likely lags behind  
366 as it is still dominated by terrestrially derived POC. ~~In smaller streams, higher water temperatures may increase  
367 activity of bacterial communities potentially resulting in stronger degradation (Adams et al., 2010). While warmer  
368 water temperatures have been shown to increase microbial degradation at a similar rate as primary production,  
369 additional supply of terrestrial OC may increase degradation rates resulting in higher CO<sub>2</sub> emissions (Demars et  
370 al., 2016).~~ ~~Furthermore~~ Similarly, [Denfeld et al., 2013 have shown that](#) leaching of terrestrial DOC and permafrost  
371 carbon may fuel stronger degradation of OC in the smaller streams than in the larger ones (Denfeld et al., 2013).

372 While larger rivers may be able to emit more greenhouse gases than smaller ones given their size, smaller  
373 rivers/streams play an important role in CO<sub>2</sub> evasion (Denfeld et al., 2013). Smaller waterways have been shown  
374 to convey more allochthonous OC-derived CO<sub>2</sub> emissions than larger rivers (Hotchkiss et al., 2015). With the  
375 predicted earlier onset of freshet and warmer temperatures occurring earlier in the season in the future (Meredith

376 et al., 2019; Stadnyk et al., 2021) (i.e., creating more favorable conditions both for primary production and OC  
377 degradation) lower order streams will largely fix CO<sub>2</sub> (by primary producers), but could also potentially increase  
378 CO<sub>2</sub> evasion via degradation of autochthonous POC ~~(that likely comprises a fraction of old permafrost OC taken~~  
379 ~~up by primary producers (Drake et al., 2018b), and/or enhance.~~ Furthermore, degradation of autochthonous POC  
380 may enhance degradation of allochthonous OC via priming effects (Hotchkiss et al., 2014). This may be  
381 particularly relevant in the Arctic, where the high proportion of allochthonous permafrost OC present during  
382 freshet could be susceptible to decomposition (Fig. 5). However, further studies are needed to decipher whether  
383 this has implications on CO<sub>2</sub> emissions in the whole system level. Furthermore, smaller rivers may transport  
384 permafrost carbon, in the form of aquatic biomass, downstream, where its signal is mixed with modern OC sources  
385 and is not detectable anymore (Drake et al., 2018b). Understanding dynamics of smaller rivers/streams is important  
386 given that river size may affect their response to environmental drivers (Battin et al., 2023). On the whole, the  
387 intensification of hydrological cycling could mean that in the future processes currently happening in lower order  
388 streams may shift towards larger fluvial systems.

## 389 **5 Conclusions and implications**

390 Here, we present seasonal contrasts, including the hydrologically important spring freshet period, in water  
391 chemistry and carbon characteristics of lower order streams and the Kolyma mainstem. However, during freshet  
392 small and mid-sized streams/rivers are more dynamic and seem to respond faster to environmental changes such as  
393 air temperature increases. While POC concentrations did not significantly differ between large and small/mid-sized  
394 rivers during freshet, composition of POC showed clear differences: the  $\delta^{13}\text{C}$ -POC was lower and POC-% higher  
395 in small and mid-sized streams/rivers than in large ones, indicating an early onset of primary production in these  
396 lower order streams. This will may result in uptake of CO<sub>2</sub> by primary producers, however, it may also fuel CO<sub>2</sub>  
397 evasion via degradation of autochthonous POC that is likely if partly comprised of allochthonous/permafrost OC  
398 (when terrestrially derived CO<sub>2</sub> is fixed by primary producers) and/or prime degradation of allochthonous OC.  
399 however, fFurther studies are needed to discern implications on CO<sub>2</sub> uptake/emissions balance on a system level.  
400 Furthermore, hydrological intensification may increase shunting and decomposition of organic matter from smaller  
401 to larger river systems, and transport permafrost-derived OC downstream in the form of autochthonous POC. An  
402 increased understanding of carbon and water chemistry of lower order streams and their linkages to hydrology is  
403 therefore crucial to understand catchment-wide OC dynamics.  
404

## 405 **Appendix A**

### 406 **Text A1. Representativeness of surface water samples**

407 As all our samples were of surface water, we compared our Kolyma River  $\delta^{13}\text{C}$ -POC data to Arctic Great Rivers  
408 Observatory (Arctic-GRO) to assess how our surface water samples would compare to depth-integrated sampling  
409 (data and sampling protocol are available in [www.arcticgreatrivers.com/data](http://www.arcticgreatrivers.com/data), water quality) carried out since 2003  
410 in the Kolyma River mainstem. All the water samples collected during 2003–2011 (programs PARTNERS,  
411 ARCTIC-GRO I) were depth-integrated, while samples collected between 2012 and 2021 (programs ARCTIC-  
412 GRO II-IV; data from 2020–2021 is provisional) are a combination of samples collected from the surface and at  
413 depth (sampled at depths of 4–15 m). The Arctic-GRO average  $\pm$  std  $\delta^{13}\text{C}$ -POC for freshet (sampled in June 2004–  
414 2021) was  $-28.2 \pm 1.4$  ‰ (n=19) and for summer (sampled in July–August 2003–2021) was  $-29.8 \pm 2.1$  ‰ (n=19).  
415 In comparison, our Kolyma River mainstem  $\delta^{13}\text{C}$ -POC sampled during freshet (June 2019) was  $-27.94 \pm 1.4$  ‰  
416 (n=6) and in summer (July–August 2018) was  $-31.44 \pm 1.5$  ‰ (n=4; table A2). Given that our  $\delta^{13}\text{C}$ -POC signature  
417 falls within the standard deviation of the depth-integrated samples we consider our samples to be sufficiently  
418 representative for the entire water column.

419

### 420 **Text A2. Endmembers for the source apportionment**

421 The endmember for autochthonous POC was according to Wild et al. (2019;  $\delta^{13}\text{C}$   $-30.6 \pm 3$  ‰, n=24), Winterfeld  
422 et al. (2015;  $\delta^{13}\text{C}$   $-30.5 \pm 2.5$  ‰, n=n/a), Levin et al. (2013;  $\Delta^{14}\text{C}$   $-39.6 \pm 5.5$  ‰, n=73) and Behnke et al. (2023;  
423  $\delta^{13}\text{C}$   $-33.1 \pm 4.7$  ‰,  $\Delta^{14}\text{C}$   $106 \pm 164$  ‰) combined with our own POC sample collected at the Panteleikha River  
424 during an algal bloom in 2019 ( $\Delta^{14}\text{C}$   $-26$  ‰;  $\delta^{13}\text{C}$   $-33.5$  ‰, n=1). The  $\delta^{13}\text{C}$  endmember values from Wild et al.,  
425 (2019) and Winterfeld et al., (2015) are of riverine phytoplankton from Ob and Yenisei rivers, and from Lena  
426 River, respectively, while the values from Levin et al. (2013) are of atmospheric  $\text{CO}_2$  (May–August 2009–2012).  
427 Endmember values from Behnke et al. (2023) are (mostly benthic) of biofilms, algae and invertebrates from  
428 Alaska, Canada, and Svalbard. As our samples were of surface water, we combined the  $\Delta^{14}\text{C}$  of atmospheric  $\text{CO}_2$   
429 from Levin et al. (2013) (following the approach used by Winterfeld et al., 2015 and Wild et al., 2019) with the  
430  $\Delta^{14}\text{C}$  of biofilms, algae, and invertebrates (following Behnke et al., 2023) as the autochthonous endmember. The  
431 autochthonous  $\delta^{13}\text{C}$  endmember was a compilation of phytoplankton (Winterfeld et al. 2015 and Wild et al. 2019)  
432 and biofilms, algae, and invertebrates (Behnke et al., 2023). For the active layer and terrestrial vegetation  
433 endmember, we used the endmembers compiled in Wild et al., (2019): endmember for active layer ( $\Delta^{14}\text{C}$   $-197.5 \pm$   
434  $148.4$  ‰, n=60;  $\delta^{13}\text{C}$   $-26.4 \pm 0.8$  ‰, n=56) and modern vegetation ( $\Delta^{14}\text{C}$   $97 \pm 124.8$  ‰, n=58;  $\delta^{13}\text{C}$   $-27.7 \pm 1.3$   
435 ‰, n=94) The active layer and terrestrial vegetation endmembers include data from Siberia, Alaska, northern  
436 Canada, and Scandinavia. For the permafrost endmember, we combined the Ice Complex Deposit ( $\Delta^{14}\text{C}$   $-954.8 \pm$   
437  $65.8$  ‰, n=329) and Holocene permafrost ( $\Delta^{14}\text{C}$   $-567.5 \pm 156.7$  ‰, n=138) endmember from Wild et al. (2019)  
438 with the Holocene permafrost endmember from Winterfeld et al. (2015;  $\Delta^{14}\text{C}$   $282 \pm 133$  ‰, n=60;  $\delta^{13}\text{C}$   $-26.6 \pm 1$   
439 ‰, n=40) and Vonk et al. (2012;  $\delta^{13}\text{C}$   $-26.3 \pm 0.7$  ‰, n=374). All endmembers were weighed with the number of  
440 observations. We recognize that having robust endmember values is important for the best modelling results, and  
441 ideally these values would come from within or close to the studied system. While the permafrost, active layer and  
442 terrestrial vegetation endmembers are relatively well defined, scientific literature lacks well-constrained  
443 autochthonous endmembers, especially for phytoplankton. Endmembers were recently discussed in Behnke et al.  
444 (2023).

445  
446  
447  
448  
449  
450  
451  
452  
453  
454  
455  
456  
457  
458  
459  
460  
461  
462  
463  
464  
465  
466  
467  
468  
469  
470  
471  
472  
473  
474  
475  
476  
477  
478  
479  
480  
481  
482  
483  
484

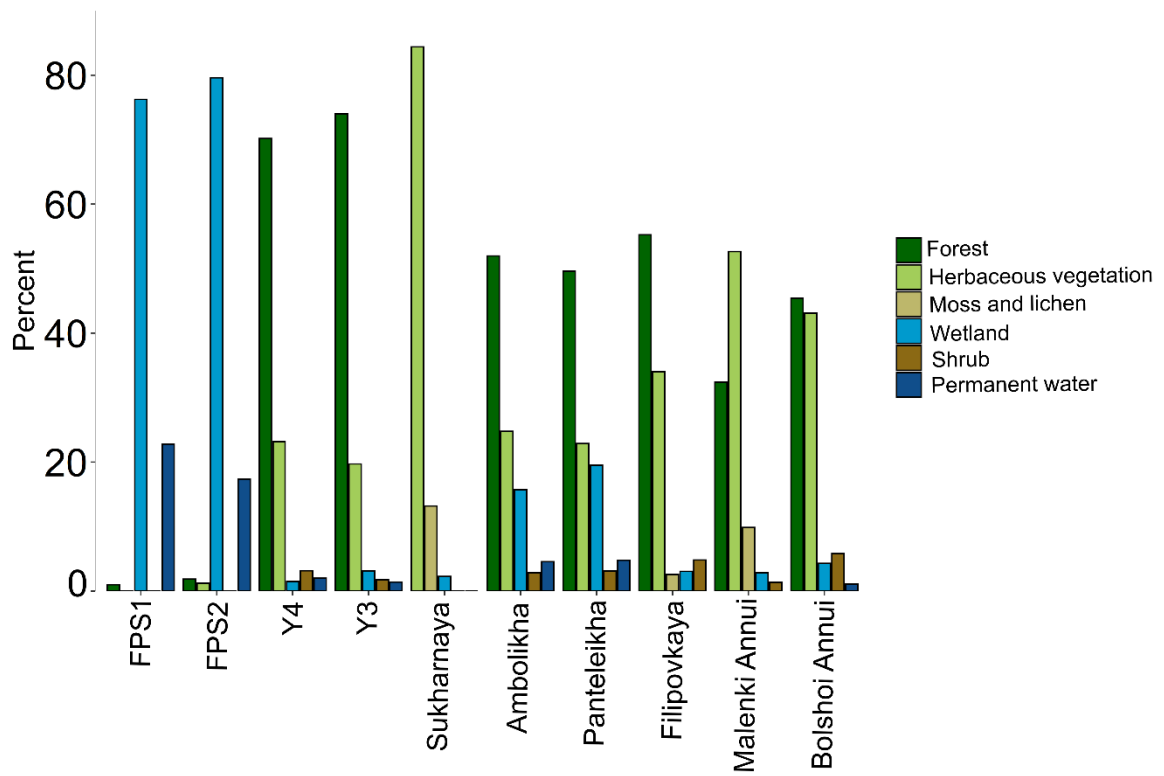
### **Text A3. Statistical analyses: assumptions and hypotheses**

For the linear regression model of water temperature and  $\delta^{13}\text{C}$ -POC;  $\delta^{13}\text{C}$ -POC and POC-%; and  $\Delta^{14}\text{C}$ -POC and POC-%, we used a function *lm*. The same function was used for linear regression of spatial parameters (slope and soil organic carbon concentration - SOCC) and OC concentrations. The POC concentrations did not show a linear relationship with the spatial parameters, thus they were not modelled. We log transformed the DOC data prior to executing the model as well as the POC-%. For all the linear regression models, we checked the assumptions of normality and homoskedasticity of the model residuals visually and using a Shapiro-Wilk test and a Breusch-Pagan test, respectively. The significance level of the test was 0.05.

To test the difference in means in water chemistry parameters (water temperature, electrical conductivity - EC, pH and  $\delta^{18}\text{O}$ ) and carbon data (POC, DOC, DIC,  $\delta^{13}\text{C}$ -OC,  $\delta^{13}\text{C}$ -DIC and  $\Delta^{14}\text{C}$ -POC) between seasons (i.e., freshet and summer) in the tributaries and the Kolyma River, we used a paired (two-sided) Welch's t-test (or Wilcoxon rank sum test if the assumptions for a paired t-test were not met). For the tributaries, n=10 for each season for each parameter except for DIC and  $\delta^{13}\text{C}$ -DIC n=8. For the Kolyma River mainstem, n=4 for each season (for freshet an average of the replicate samples at sites K3 and K4 were used) except for DIC and  $\delta^{13}\text{C}$ -DIC n=3. Our H0 hypothesis was that the means are equal between seasons and the H1 hypothesis that the means are not equal. The test significance level was 0.05. We checked the normality of the differences data by using the Shapiro-Wilk test, and log transformed the data in case of non normality. For  $\Delta^{14}\text{C}$  POC of tributaries, a Mann-Whitney U test was used.

To test whether there was a significant difference between small streams, midsized rivers, and large rivers regarding carbon parameters (POC, DOC, DIC,  $\delta^{13}\text{C}$ -OC,  $\delta^{13}\text{C}$ -DIC and  $\Delta^{14}\text{C}$ -POC), we used (one-way) analysis of variance (ANOVA) or a Kruskal-Wallis test (when assumptions for ANOVA were not met) for each season separately. The floodplain streams (FPS1 and FPS2), Y3 and Y4 were classed as small streams; Panteleikha, Ambolikha, Filipovkaya and Sukarnaya as midsized rivers; and Malenki Annu, Bolshoi Annu and Kolyma mainstem as large rivers. For the small and midsized rivers during freshet, n=4 while for large rivers n=6 for each parameter. For the summer, n=4 for each parameter in small and midsized rivers, and n=6 in large rivers except for DIC and  $\delta^{13}\text{C}$ -DIC n=3 in small and midsized rivers and n=5 in large rivers. We checked the assumptions of normality and equal variances visually and further with Shapiro-Wilk test and Breusch-Pagan test, respectively. Our H0 hypothesis was that the means are equal between different sized rivers/streams and the H1 hypothesis that the means are not all equal. With significant results, we used a Tukey's test as a *post hoc* test for ANOVA and a Dunn's test for the Kruskal-Wallis test. The significance level of all the tests was 0.05.

~~For the linear regression model of water temperature and  $\delta^{13}\text{C}$ -POC;  $\delta^{13}\text{C}$ -POC and POC-%; and  $\Delta^{14}\text{C}$ -POC and POC-%, we used a function *lm*. The same function was used for linear regression of spatial parameters (slope and soil organic carbon concentration - SOCC) and OC concentrations. The POC concentrations did not show a linear relationship with the spatial parameters, thus they were not modelled. We log transformed the DOC data prior to executing the model as well as the POC-%. For all the linear regression models, we checked the assumptions of normality and homoskedasticity of the model residuals visually and using a Shapiro-Wilk test and a Breusch-Pagan test, respectively. The significance level of the test was 0.05. All the statistical testing was executed in R (R Core Team, 2020).~~



485 **Figure A1.** Land cover of the tributary watersheds. The watersheds are organized by their size starting from the smallest (FPS1)  
 486 on the left. The land cover types with < 1 % contribution are not included in the figure, see Table A5 for full land cover data.  
 487  
 488

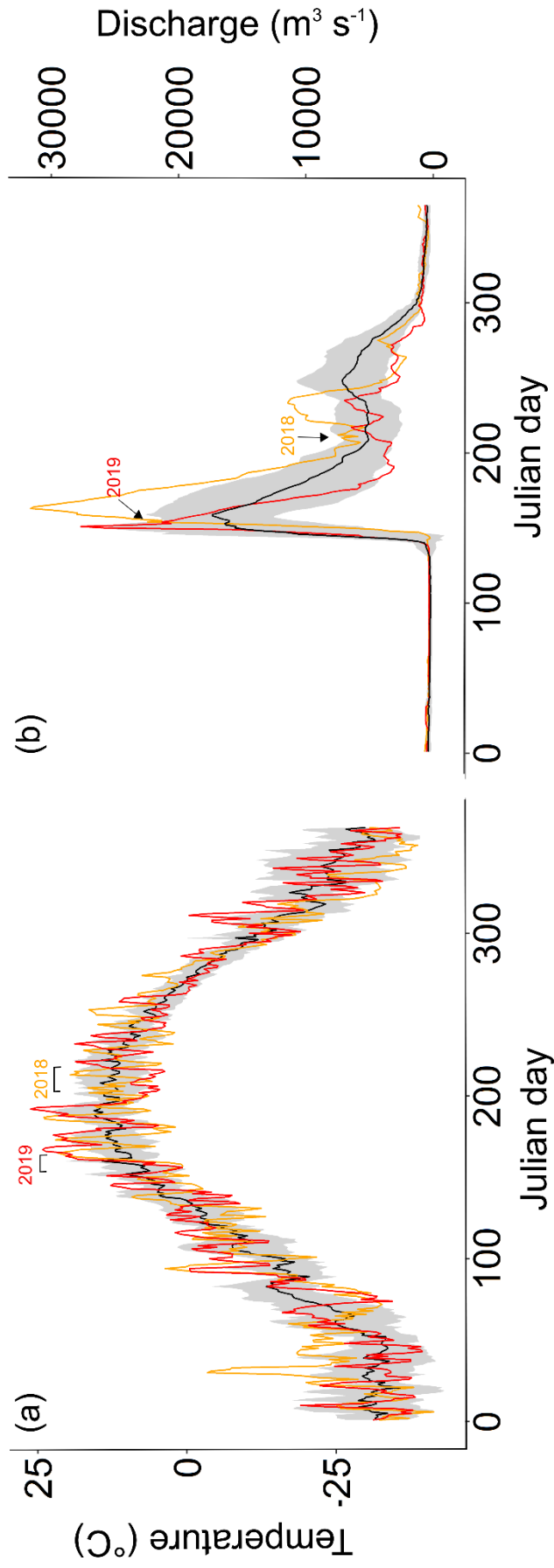
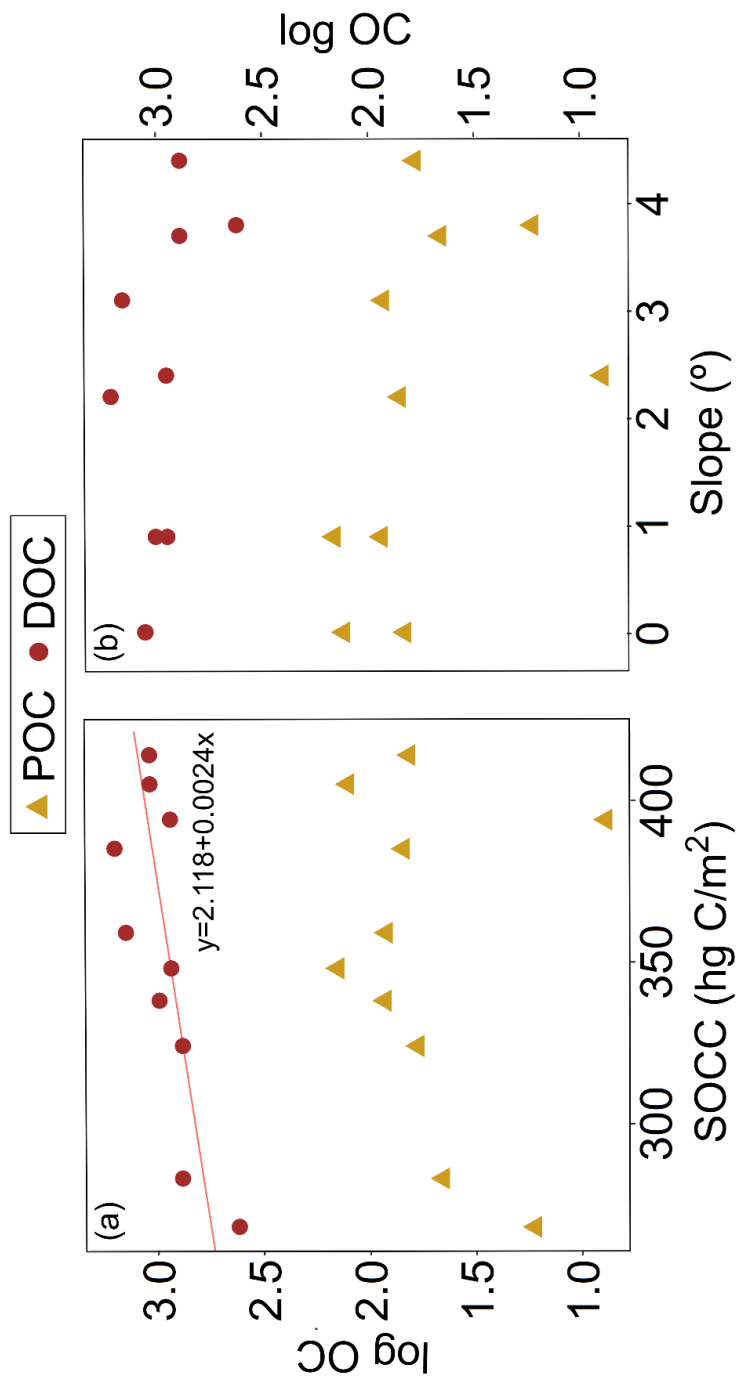


**Figure A2.** (a) average air temperature  $\pm$  standard deviation (black line  $\pm$  grey background) 2007–2017 in Cherskiy with air temperatures during the sampling years 2018 (orange line) and 2019 (red line). The weather data was retrieved from the Cherskiy weather station. Timing of the sampling campaigns is marked above the plot. See Table S3 for air temperatures on sampling days. (b) The average  $\pm$  standard deviation of discharge measured at Kolymnskoye 2007–2017 (Shiklomanov et al., 2021). Red line shows the discharge of the year 2019 and orange line the year 2018. The timing of the sampling campaigns is marked with arrows above the plot.

489  
 490  
 491  
 492  
 493  
 494



495  
 496 **Figure A3.** (a) Particulate and dissolved organic carbon (POC and DOC, respectively) concentration (log) and soil organic carbon content (SOCC). Linear regression for DOC was statistically  
 497 significant ( $R^2 = 0.49$ ,  $F(1,8) = 9.59$ ,  $p = 0.001$ ). (b) Concentrations (log) of POC and DOC against median slope. The regression model did not show statistically significant results. All the organic  
 498 carbon data are from the Kolyma River tributaries sampled during summer 2018.

499 **Table A1.** Sampling coordinates and dates of the Kolyma tributaries and Kolyma mainstem during spring freshet (2019) and  
500 summer (2018) sampling campaigns. Data from sites KOL1–KOL4 during freshet and KOL1–KOL3 during summer were  
501 previously reported in Keskitalo et al. (2022).  
502

<b>Freshet</b>	<b>Latitude</b>	<b>Longitude</b>	<b>Sampling date (dd/mm/yyyy)</b>
FPS1	N68.65100	E161.36472	18/06/2019
FPS2	N68.64977	E161.36742	18/06/2019
Y4	N68.74133	E161.41393	08/06/2019
Y3	N68.75919	E161.44769	09/06/2019
Sukharnaya	N69.49534	E161.83316	11/06/2019
Ambolikha	N68.66421	E161.38884	14/06/2019
Panteleikha	N68.70052	E161.52057	10/06/2019
Filipovkaya	N68.92067	E161.64552	16/06/2019
Malenki Annui	N68.47034	E160.83749	07/06/2019
Bolshoi Annui	N68.46519	E160.80356	07/06/2019
KOL1	N68.51782	E160.98093	07/06/2019
KOL2	N68.66630	E161.19991	07/06/2019
KOL3	N69.20045	E161.44044	11/06/2019
KOL4	N69.62680	E162.21594	11/06/2019
KOL3re*	N69.20045	E161.44044	16/06/2019
KOL4re*	N69.62680	E162.21594	16/06/2019
<b>Summer</b>			
FPS1	N68.65108	E161.36438	07/08/2018
FPS2	N68.64903	E161.36606	09/08/2018
Y4	N68.74216	E161.41379	04/08/2018
Y3	N68.75919	E161.44769	26/07/2018
Sukharnaya	N69.49577	E161.83197	28/07/2018
Ambolikha	N68.67504	E161.41608	21/07/2018
Panteleikha	N68.67068	E161.52295	30/07/2018
Filipovkaya	N68.90665	E161.68976	06/08/2018
Malenki Annui	N68.45193	E160.81279	01/08/2018
Bolshoi Annui	N68.46015	E160.78267	01/08/2018
KOL1	N68.50713	E160.61034	23/07/2018
KOL2	N68.75443	E161.27150	25/07/2018
KOL3	N69.20045	E161.44044	28/07/2018
KOL4	N69.32058	E161.56134	28/07/2018

\*repeat measurement.

503



504 **Table A2.** Concentrations of total suspended solids (TSS), particulate and dissolved organic carbon (POC and DOC, respectively), dissolved inorganic carbon (DIC) in the Kolyma River during  
505 freshet (June 2019) and summer (July–Aug 2018). Also shown are stable isotopes of carbon:  $\delta^{13}\text{C}$  of POC, DOC and DIC, and concentrations of total particulate nitrogen (TPN) and molar ratio of  
506 POC/TPN. For  $\Delta^{14}\text{C}$ -POC, see Table A7. Mean and standard deviation between replicate samples (n=4) is shown for freshet sites KOL1-KOL4 and for summer KOL1-KOL3 (n=3, KOL3 n=4)  
507 including analytical uncertainty for DIC and  $\delta^{13}\text{C}$ -DIC. For KOL3re and KOL4re n=1. For water isotopes ( $\delta^{18}\text{O}$ ,  $\delta\text{H}$ ) and summer DIC and  $\delta^{13}\text{C}$ -DIC only analytical error (no replicates) is shown.  
508 All data from KOL1–KOL4 during freshet and KOL1–KOL3 during summer (except DIC concentrations) were previously published in Keskitalo et al. (2022).

Site	TSS (mg L <sup>-1</sup> )	POC ( $\mu\text{M}$ )	POC (%)	$\delta^{13}\text{C}$ -POC (%)	TPN ( $\mu\text{M}$ )	POC/ TPN	DOC ( $\mu\text{M}$ )	$\delta^{13}\text{C}$ -DOC (%)	DIC ( $\mu\text{M}$ )	$\delta^{13}\text{C}$ -DIC (%)	$\delta^{18}\text{O}$ (%)	$\delta\text{H}$ (%)	
Freshet	KOL1	51±2	103±5	2.4±0.2	-26.77±0.2	9.03±0.4	9.8±0.3	731±7	-26.36±0.2	294±18	-12.19±0.16	-22.89±0.09	-178.4±0.6
	KOL2	63±5	126±4	2.4±0.2	-27.04±0.2	10.9±0.6	10±0.3	764±11	-26.42±0.2	239±16	-13.77±0.09	-22.88±0.22	-176.5±1.4
	KOL3	68±2	130±5	2.3±0.1	-27.15±0.2	11.0±0.5	10±0.3	694±8	-27.11±0.2	324±10	-13.81±0.36	-22.65±0.05	-174.5±0.2
	KOL4	25±2	87.4±5	4.2±0.4	-28.10±0.2	8.13±0.5	9.2±0.3	776±11	-26.89±0.1	273±8	-13.62±0.04	-22.99±0.02	-177.1±0.4
	KOL3re	14	42.8	7.0	-28.01	3.92	9.4	574	-26.57	n/a	n/a	-26.57±0.26	-174.5±1.5
	KOL4re	10	60.1	3.3	-30.57	6.35	8.1	710	-26.84	285±0.7	-12.07±0.1	-26.84±0.25	-169.3±1.5
Summer	KOL1	9.8	42.6±3	4.8	-33.01±0.4	4.93±0.4	7.4±0.2	262±5	-29.37±0.2	470±0.1	-9.36±0.02	-22.14±0.03	-171.7±0.7
	KOL2	12±1	48.6±2	5.0±0.3	-32.32±0.6	6.20±0.3	6.7±0.1	272±15	-29.31±0.3	531±0.1	-9.46±0.04	-22.10±0.04	-171.5±0.3
	KOL3	21±4	56.8±9	3.3±0.1	-29.67±0.3	5.63±0.6	8.6±0.5	278±19	-29.46±0.6	419±0.2	-9.08±0.02	-21.36±0.03	-165.5±0.1
	KOL4	18	59.0	3.9	-30.75	6.72	7.5	269	-28.83	n/a	n/a	-21.53±0.02	-166.9±1.9

509

510

511 **Table A3.** Water chemistry parameters including water temperature (Water temp), dissolved oxygen (DO), electrical  
512 conductivity (EC) and pH in the Kolyma River and its tributary streams/rivers during freshet (early June 2019) and summer  
513 (July–Aug 2018). Also shown is air temperature (Air temp) on the sampling day measured at Cherskiy weather station. All  
514 data from KOL1–KOL4 during freshet and KOL1–KOL3 during summer were previously published in Keskitalo et al. (2022).  
515

<b>Freshet</b>	<b>Water temp</b> (° C)	<b>DO</b> (mg L <sup>-1</sup> )	<b>EC</b> (µM cm <sup>-1</sup> )	<b>pH</b>	<b>Air temp</b> (° C)
FPS1	20.9	3.43	46.5	7.74	19.6
FPS2	21.0	7.48	55.5	7.21	19.6
Y4	8.8	10.2	48.4	8.77	4.9
Y3	7.3	10.8	43.4	7.90	14.1
Sukharnaya	15.1	9.7	25.2	6.93	19.3
Ambolikha	14.9	7.77	48.3	7.23	21.2
Panteleikha	10.9	9.12	46	7.00	18.9
Filipovkaya	20.8	8.81	42	n/a	24.3
Malenki Annui	6.87	10.0	41.6	6.87	7.6
Bolshoi Annui	6.70	10.1	42.1	7.06	7.6
KOL1	7.70	10.5	102.00	7.10	7.6
KOL2	7.20	10.4	73.10	6.92	7.6
KOL3	9.80	9.86	68.70	6.65	19.3
KOL4	9.30	10.1	81.70	7.09	19.3
KOL3re*	13.8	9.39	104	n/a	24.3
KOL4re*	17.6	9.45	78	n/a	24.3
<b>Summer</b>	<b>Temp</b> (° C)	<b>DO</b> (mg L <sup>-1</sup> )	<b>EC</b> (µM cm <sup>-1</sup> )	<b>pH</b>	<b>Air temp</b> (° C)
FPS1	12.8	3.73	139	6.61	4.2
FPS2	13.3	9.08	180	7.26	10.1
Y4	11.2	6.36	271	7.17	14.6
Y3	12.3	6.29	211	6.98	12.8
Sukharnaya	8.5	9.63	75	7.77	7.8
Ambolikha	15.5	7.83	134	7.32	17.1
Panteleikha	14.3	8.32	139	6.93	9.2
Filipovkaya	17.0	10.1	162	7.47	7.6
Malenki Annui	14.0	9.41	185	7.09	19.1
Bolshoi Annui	13.0	8.95	169	7.06	19.1
KOL1	15.2	9.25	255	7.69	19.4
KOL2	15.0	9.43	249	7.16	13.2
KOL3	13.3	9.00	222	7.48	7.8
KOL4	12.5	9.16	228	7.25	7.8

\*repeat samples of KOL3 and KOL4 taken on the 16<sup>th</sup> of June 2019.

516

517

518

519 **Table A4.** Watershed size, slope and soil organic carbon content (SOCC) in the top 100 cm (Hugelius et al., 2013). Slope and  
 520 SOCC are shown as mean  $\pm$  standard deviation, also the slope median is shown.  
 521

<b>River/stream</b>	<b>Watershed size (km<sup>2</sup>)</b>	<b>Slope mean (°)</b>	<b>Slope median (°)</b>	<b>Mean SOCC (hg C/m<sup>2</sup>)</b>
FPS1	0.33	0.01 $\pm$ 0	0.01	405 $\pm$ 10
FPS2	0.74	0.01 $\pm$ 0	0.01	414
Y4	2.48	2.3 $\pm$ 1.6	2.4	394 $\pm$ 11
Y3	36.09	2.8 $\pm$ 3.3	2.2	385 $\pm$ 3
Sukharnaya	956.0	5.7 $\pm$ 5.6	3.8	269 $\pm$ 124
Ambolikha	1234	2.6 $\pm$ 4.9	0.9	338.3 $\pm$ 116
Panteleikha	1782	2.5 $\pm$ 4.6	0.9	355 $\pm$ 103
Filipovkaya	1966	4.4 $\pm$ 4.2	3.1	357 $\pm$ 99
Malenki Annui	49754	7.0 $\pm$ 7.4	4.4	319 $\pm$ 103
Bolshoi Annui	56636	6.2 $\pm$ 7.1	3.7	281 $\pm$ 113
Kolyma*	657171	7.8 $\pm$ 14	5.3	290 $\pm$ 188

522 \*Kolyma delineation from Shiklomanov et al. (2021).

523

524 **Table A5.** Land cover types per watershed in percentages (%). Land cover classes are according to Buchhorn et al. (2020).  
 525

<b>River/Stream</b>	<b>Forest</b>	<b>Wetland</b>	<b>Shrubs</b>	<b>Herbaceous vegetation</b>	<b>Permanent Water</b>	<b>Moss and lichen</b>	<b>Bare sparse vegetation</b>	<b>Urban built</b>
FPS1	1	76	0	0	23	0	0	0
FPS2	2	80	0	1	17	0	0	0
Y4	70	1	3	23	2	0	0	0
Y3	74	3	2	20	1	0	0	0
Sukharnaya	0	2	<1	84	<1	13	0	0
Ambolikha	52	16	3	25	5	<1	0	0
Panteleikha	50	20	3	23	5	<1	0	<1
Filipovkaya	55	3	5	34	<1	3	0	0
Malenki Annui	32	3	1	53	<1	10	<1	<1
Bolshoi Annui	45	4	6	43	1	<1	<1	<1

526

527

**Table A6.** Paired ~~Welch's~~-t-test results for difference in means in electrical conductivity (EC), water temperature (Temp), pH, water isotope  $\delta^{18}\text{O}$ , total suspended solids (TSS), particulate and dissolved organic carbon (POC and DOC), dissolved inorganic carbon (DIC),  $\delta^{13}\text{C}$  of POC, DOC and DIC and  $\Delta^{14}\text{C}$ -POC between seasons (freshet and summer) in the Kolyma mainstem and its tributaries. The significantly different results are highlighted in bold. The significance level was 0.05. For TSS, Wilcoxon signed rank test was used. For tributaries,  $n=10$  for all parameters except for DIC and  $\delta^{13}\text{C}$ -DIC  $n=8$  for each season. For  $\Delta^{14}\text{C}$  in tributaries, Mann-Whitney U-test was used. See more details in [Text A3 the supplementary methods](#).

Site	EC	Temp	$\delta^{18}\text{O}$	TSS	POC	$\delta^{13}\text{C}$ -POC	$\Delta^{14}\text{C}$	TPN	DOC	$\delta^{13}\text{C}$ -DOC	DIC	$\delta^{13}\text{C}$ -DIC
Tributaries	$t(9.4)=$	$t(11.6)=$	$t(18.4)=$	$t(17.7)=$	$t(17.7)=$	$t(17.3)=$	$U=79$	$t(17.7)=$	$t(17.0)=$	$t(15.0)=$	$t(13.6)=$	$t(15.0)=$
	7.36	-0.07	7.19	-0.92	-0.76	-1.13	<b><math>p&lt;0.029</math></b>	-0.434	-1.21	-4.6	3.86	4.28
	<b><math>p&lt;0.001</math></b>	$p=0.946$	<b><math>p&lt;0.001</math></b>	$p=0.371$	$p=0.457$	$p=0.274$	$t(3.7)=$	$p=0.669$	$p=0.242$	<b><math>p&lt;0.001</math></b>	<b><math>p&lt;0.005</math></b>	<b><math>p&lt;0.001</math></b>
Kolyma	$t(6.2)=$	$t(6.4)=$	$t(8.0)=$	$t(5.6)=$	$t(5.7)=$	$t(6.2)=$	$t(3.7)=$	$t(6.1)=$	$t(5.1)=$	$t(6.8)=$	$t(2.8)=$	$t(3.3)=$
	-15.3	-1.8	-2.33	2.22	2.69	3.7	-0.1	1.989	14.6	13.6	-5.4	-7.4
	<b><math>p&lt;0.005</math></b>	$p=0.126$	<b><math>p=0.048</math></b>	$p=0.071$	<b><math>p=0.04</math></b>	<b><math>p=0.01</math></b>	$p=0.94$	$p=0.093$	<b><math>p&lt;0.005</math></b>	<b><math>p&lt;0.005</math></b>	<b><math>p=0.015</math></b>	<b><math>p=0.004</math></b>
Site	EC	Temp	$\delta^{18}\text{O}$	TSS	POC	$\delta^{13}\text{C}$ -POC	$\Delta^{14}\text{C}$	TPN	DOC	$\delta^{13}\text{C}$ -DOC	DIC	$\delta^{13}\text{C}$ -DIC
Tributaries	$t(9)=$	$t(9)=$	$t(9)=$	$V(17.7)=$	$t(9)=$	$t(9)=$	$t(9)=$	$t(9)=$	$t(9)=$	$t(9)=$	$t(7)=$	$t(7)=$
	8.0876	-0.06892	6.4858	12	-0.90069	-1.1462	2.6623	-0.549	-1.5625	-5.8024	4.4603	4.9646
Kolyma	<b><math>p&lt;0.001</math></b>	$p=0.9466$	<b><math>p&lt;0.001</math></b>	$p=0.1309$	$p=0.391$	$p=0.281$	<b><math>p&lt;0.026</math></b>	$p=0.599$	$p=0.153$	<b><math>p&lt;0.001</math></b>	<b><math>p&lt;0.003</math></b>	<b><math>p&lt;0.002</math></b>
	$t(3)=$	$t(3)=$	$t(3)=$	$t(3)=$	$t(3)=$	$t(3)=$	$t(3)=$	$t(3)=$	$t(3)=$	$t(3)=$	$t(2)=$	$t(2)=$
	-18.212	-1.815	-7.7009	2.4477	3.1987	3.1791	-0.0671	2.8703	14.39	11.266	-3.2828	-6.8875
	<b><math>p&lt;0.001</math></b>	$p=0.167$	<b><math>p=0.006</math></b>	$p=0.09$	<b><math>p=0.049</math></b>	$p=0.05$	$p=0.95$	$p=0.06$	<b><math>p=0.001</math></b>	<b><math>p=0.002</math></b>	$p=0.08$	<b><math>p=0.02</math></b>

528  
529  
530  
531  
532

533

534  
535

536 **Table A7.** Fractions (%) of different carbon pools, particulate organic carbon (POC), dissolved organic carbon (DOC) and  
 537 dissolved inorganic carbon (DIC), during freshet (June 2019) and summer (July–August 2018).  
 538

<b>River/Stream</b>	<b>Freshet</b>			<b>Summer</b>		
	<b>POC</b>	<b>DOC</b>	<b>DIC</b>	<b>POC</b>	<b>DOC</b>	<b>DIC</b>
Floodplain	3.66	76.4	30.2	7.01	61.4	31.6
Headwater	3.53	81.3	15.1	0.42	70.7	28.9
Wetland	6.26	72.7	21.0	8.76	61.8	29.5
Tundra	10.2	69.8	20.0	9.94	43.6	46.5
Forest	8.44	75.9	15.7	7.56	53.3	39.2
Kolyma	9.05	65.7	25.3	6.24	34.2	59.6

539

**Table A8.** Analysis of variance (ANOVA) and Kruskal-Wallis test results for difference in means in total suspended solids (TSS), particulate and dissolved organic carbon (POC and DOC), total particulate nitrogen (TPN), dissolved inorganic carbon (DIC),  $\delta^{13}\text{C}$  of POC, DOC and DIC and  $\Delta^{14}\text{C}$ -POC between small rivers (FPS1, FPS2, Y3, Y4), midsize (mid) rivers (Panteleikha, Ambolikha, Sukharnaya, Filipovkaya) and large rivers (Malenki Annui, Bolshoi Annui and Kolyoma mainstem) during freshet and summer separately with F statistics (from ANOVA) or H statistics (from Kruskal-Wallis test), degrees of freedom and p-values. The statistically significant ( $p < 0.05$ ) results are highlighted in bold. When ANOVA or Kruskal-Wallis test results were significant, post hoc test (Tukey's test for ANOVA and Dunn's test for the Kruskal-Wallis test) was conducted and their results (p-values) are listed below to indicate whether the difference was significant, small and midsize rivers, small and large rivers and/or midsize and large rivers (n/a indicates not applicable when post hoc test was not executed due to ANOVA or Kruskal-Wallis test not showing significant results). See more details in [Text A.3 the supplementary methods](#).

	<b>TSS</b>	<b>POC</b>	<b>POC-%</b>	<b><math>\delta^{13}\text{C}</math>-POC</b>	<b><math>\Delta^{14}\text{C}</math></b>	<b>TPN</b>	<b>DOC</b>	<b><math>\delta^{13}\text{C}</math>-DOC</b>	<b>DIC</b>	<b><math>\delta^{13}\text{C}</math>-DIC</b>
<b>Freshet</b>	H(2)= <b>11.046</b>	H(2)= 4.9632	H(2)= <b>10.649</b>	H(2)= <b>9.9265</b>	H(2)= 3.8	F(4,3,2)= 2.559	H(2)= <b>7.7646</b>	H(2)= <b>7.1471</b>	F(12,2)= 0.033	H(2)= 1.0571
Small-mid	p=1.000	n/a	p=1.000	p=1.00	n/a	n/a	p=0.704	p=1.000	n/a	n/a
Small-large	p=0.007	n/a	p=0.034	p=0.03	n/a	n/a	p=0.018	p=0.369	n/a	n/a
Mid-large	p=0.069	n/a	p=0.016	p=0.03	n/a	n/a	p=0.510	p=0.030	n/a	n/a
<b>Summer</b>	H(2)=	H(2)=	H(2)=	F(11,2)=	H(2)=	H(2)=	H(2)=	H(2)=	F(8,2)=	F(8,2)=
Small-mid	2.881	1.3143	8.8238	1.261	<b>6.9238</b>	2.581	<b>10.881</b>	1.6952	1.453	1.016
Small-large	p=0.2368	p=0.5183	p=0.0121	p=0.321	p=0.031	p=0.2751	p=0.004	p=0.4284	p=0.29	p=0.404
Mid-large	n/a	n/a	p=1.000	n/a	p=1.000	n/a	p=0.452	n/a	n/a	n/a
Small-mid	n/a	n/a	p=0.044	n/a	p=0.044	n/a	p=0.003	n/a	n/a	n/a
Small-large	n/a	n/a	p=0.034	n/a	p=0.179	n/a	p=0.269	n/a	n/a	n/a
Mid-large	n/a	n/a	p=0.048	n/a	p=0.048	n/a	p=0.033	p=0.025	p=0.939	p=0.5894
<b>Freshet</b>	H(2)= <b>10.057</b>	H(2)= <b>6.1143</b>	H(2)= <b>9.7143</b>	H(2)= <b>8.8283</b>	H(2)= 3.8	F(11,2)= 3.527	H(2)= <b>6.8</b>	H(2)= <b>7.381</b>	F(11,2)= 0.063	H(2)= 1.0571
Small-mid	p=0.007	p=0.047	p=0.008	p=0.012	p=0.1496	p=0.0655	p=0.033	p=0.025	p=0.939	p=0.5894
Small-large	p=1.000	n/a	p=1.000	p=1.00	n/a	n/a	p=0.710	p=1.000	n/a	n/a
Mid-large	p=0.001	p=0.048	p=0.016	p=0.04	n/a	n/a	p=0.029	p=0.269	n/a	n/a
<b>Summer</b>	H(2)=	H(2)=	H(2)=	F(11,2)=	H(2)=	H(2)=	H(2)=	H(2)=	F(8,2)=	F(8,2)=
Small-mid	2.881	1.3143	8.8238	1.261	<b>6.9238</b>	2.581	<b>10.881</b>	1.6952	1.453	1.016
Small-large	p=0.2368	p=0.5183	p=0.0121	p=0.321	p=0.031	p=0.2751	p=0.004	p=0.4284	p=0.29	p=0.404
Mid-large	n/a	n/a	p=1.000	n/a	p=1.000	n/a	p=0.452	n/a	n/a	n/a
Small-mid	n/a	n/a	p=0.044	n/a	p=0.044	n/a	p=0.003	n/a	n/a	n/a
Small-large	n/a	n/a	p=0.034	n/a	p=0.179	n/a	p=0.269	n/a	n/a	n/a
Mid-large	n/a	n/a	p=0.048	n/a	p=0.048	n/a	p=0.033	p=0.026	p=0.939	p=0.5894

550 **Table A9.** Radiocarbon measurements for particulate organic carbon (POC) including the fraction modern (Fm),  $\Delta^{14}\text{C}$  and uncalibrated  $^{14}\text{C}$   
551 ages. The ETH code is a unique analysis ID assigned for each sample analyzed at the Laboratory of Ion Beam Physics, ETH, Zürich. The  
552 uncertainties are according to the method described in Haghypour et al. (2019).  
553

	Site	ETH code	Fm	$\Delta^{14}\text{C}$	Age (yrs)
<b>Freshet</b>	FPS1	105814.1.1	0.55±0.01	-454	4800
	FPS2	105803.1.1	0.74±0.02	-268	2434
	Y4	105809.1.1	0.88±0.01	-122	982
	Y3	105811.1.1	0.77±0.01	-239	2132
	Sukharnaya	105804.1.1	0.79±0.01	-220	1927
	Ambolikha	105810.1.1	0.88±0.02	-132	1070
	Panteleikha	105813.1.1	0.94±0.02	-65	473
	Filipovkaya	105817.1.1	0.74±0.01	-265	2410
	Malenki Annui	105808.1.2	0.72±0.01	-284	2613
	Bolshoi Annui	n/a	0.58±0.17	-291	2694
	KOL1	105801.1.1	0.62±0.01	-385	3844
	KOL1 replicate 1	105813.1.2	0.68±0.01	-321	3047
	KOL2	105811.1.2	0.66±0.01	-347	3361
	KOL2 replicate 1	105814.1.2	0.67±0.01	-332	3172
	KOL3	105802.1.1	0.94±0.01	-69	504
	KOL4	105800.1.1	0.70±0.01	-302	2820
	KOL3re	105815.1.1	0.65±0.01	-353	3436
	KOL4re	105806.1.1	0.63±0.01	-380	3774
<b>Summer</b>	FPS1	106134.1.1	0.97±0.01	-38	246
	FPS2	106135.1.1	0.96±0.01	-52	365
	Y4	106128.1.1	0.97±0.02	-43	285
	Y3	102311.1.1	0.83±0.01	-177	1499
	Sukharnaya	102304.1.1	0.73±0.01	-274	2503
	Ambolikha	102320.1.1	0.94±0.01	-63	458
	Panteleikha	102305.1.1	0.98±0.01	-24	128
	Filipovkaya	102313.1.1	0.94±0.01	-63	456
	Malenki Annui	102317.1.1	0.66±0.01	-348	3368
	Bolshoi Annui	102318.1.1	0.83±0.01	-175	1477
	KOL1	104321.1.1	0.78±0.02	-231	2040
	KOL1 replicate 1	102314.1.1	0.79±0.01	-213	1855
	KOL1 replicate 2	102315.1.1	0.79±0.01	-208	1806
	KOL2	101944.1.1	0.80±0.01	-205	1781
	KOL2 replicate 1	101945.1.1	0.78±0.01	-222	1953
	KOL2 replicate 2	101946.1.1	0.77±0.01	-239	2131
	KOL3	102301.1.1	0.70±0.01	-306	2869
	KOL4	104322.1.1	0.71±0.01	-296	2748

554



555 **Table A10.** Sampling date, concentrations of dissolved organic carbon (DOC) and  $\Delta^{14}\text{C}$ -DOC of floodplain stream (FPS), Y4, Y3 and  
556 Panteleikha sampled during 2006–2011 (previously unpublished data; all sampling by Anya Davydova and Sergei Davydov). The location  
557 of FPS is N68.73515, E161.40408, thus different from FPS locations in this study. The ETH code is a unique analysis ID assigned for each  
558 sample analyzed at the Laboratory of Ion Beam Physics, ETH, Zürich.  
559

Site	Sampling date (dd/mm/yyyy)	DOC ( $\mu\text{M}$ )	ETH code	$\Delta^{14}\text{C}$ (‰)
FPS	06/10/2010	n/a	47880.1.1	57.4
FPS	06/09/2011	613	48172.1.1	69.7
FPS	28/09/2011	483	48165.1.1	71.1
Y4	05/10/2006	1239	48359.1.1	18.2
Y4	15/06/2007	1424	48358.1.1	61.9
Y4	31/07/2007	1837	47879.1.1	23.5
Y4	07/08/2007	2348	47877.1.1	91.2
Y4	16/08/2007	2182	47875.1.1	75.6
Y4	25/09/2007	1825	47874.1.1	62.4
Y4	10/05/2010	n/a	48368.1.1	121
Y4	04/09/2010	n/a	48356.1.1	78.0
Y4	11/09/2010	n/a	47876.1.1	78.7
Y4	04/10/2010	n/a	47878.1.1	56.7
Y4	18/08/2011	1358	48174.1.1	34.2
Y4	06/09/2011	1015	48162.1.1	36.3
Y4	18/09/2011	2116	48164.1.1	81.4
Y4	28/09/2011	1517	48171.1.1	72.4
Y3	05/10/2006	1544	48362.1.1	49.2
Y3	15/06/2007	1550	48357.1.1	64.9
Y3	31/07/2007	2220	47885.1.1	13.7
Y3	07/08/2007	1691	47884.1.1	60.5
Y3	16/08/2007	1717	47883.1.1	55.6
Y3	02/10/2007	n/a	47886.1.1	96.6
Y3	02/10/2007	1719	47881.1.1	80.5
Y3	10/05/2010	n/a	48366.1.1	123
Y3	02/09/2010	n/a	48367.1.1	87.1
Y3	04/09/2010	n/a	48365.1.1	54.5
Y3	18/08/2011	1402	48168.1.1	67.6
Y3	05/09/2011	1310	48163.1.1	63.2
Y3	11/09/2011	n/a	47882.1.1	82.6
Y3	18/09/2011	1620	48173.1.1	81.5
Y3	27/09/2011	1385	48169.1.1	73.6
Panteleikha	18/08/2011	802	48170.1.1	33.3
Panteleikha	06/09/2011	336	48360.1.1	-5.1
Panteleikha	19/09/2011	546	48161.1.1	24.4
Panteleikha	28/09/2011	455	48176.1.1	23.2

560

561

562

563 **Table A11.** Source apportionment results from Markov Chain Monte Carlo analysis showing mean, standard deviation (SD) and quantiles  
564 (2.5%, 5%, 25%, 75%, 95% and 97.5%) of particulate organic carbon (POC) from active layer, permafrost, autochthonous and terrestrial  
565 vegetation (terrestrial veg) sources during freshet and summer in floodplain (FPS), headwater, wetland, tundra, forest and Kolyma mainstem.  
566 For endmembers and further details, see supplementary methods.

	Watershed	Source	Mean	SD	2.50%	5%	25%	50%	75%	95%	97.50%
<b>Freshet</b>	FPS	Active layer	0.085	0.092	0.002	0.003	0.020	0.055	0.118	0.276	0.338
		Permafrost	0.243	0.100	0.054	0.075	0.176	0.245	0.310	0.410	0.445
		Autochthonous	0.632	0.119	0.386	0.431	0.556	0.637	0.712	0.817	0.853
		Terrestrial veg	0.039	0.050	0.000	0.001	0.007	0.021	0.052	0.139	0.173
	Headwater	Active layer	0.150	0.148	0.002	0.004	0.034	0.104	0.227	0.468	0.525
		Permafrost	0.175	0.090	0.031	0.044	0.108	0.168	0.234	0.332	0.365
		Autochthonous	0.597	0.161	0.255	0.316	0.489	0.608	0.717	0.841	0.880
		Terrestrial veg	0.078	0.104	0.000	0.001	0.009	0.034	0.106	0.305	0.377
	Wetland	Active layer	0.061	0.068	0.001	0.002	0.013	0.035	0.086	0.201	0.244
		Permafrost	0.081	0.055	0.009	0.014	0.039	0.069	0.110	0.186	0.211
		Autochthonous	0.821	0.102	0.576	0.625	0.763	0.839	0.897	0.955	0.968
		Terrestrial veg	0.037	0.057	0.000	0.001	0.005	0.015	0.044	0.157	0.203
	Tundra	Active layer	0.327	0.122	0.076	0.117	0.241	0.334	0.413	0.519	0.555
		Permafrost	0.335	0.144	0.092	0.117	0.225	0.324	0.436	0.584	0.634
		Autochthonous	0.095	0.122	0.001	0.001	0.009	0.038	0.138	0.364	0.435
		Terrestrial veg	0.026	0.032	0.001	0.001	0.006	0.015	0.034	0.088	0.116
	Forest	Active layer	0.138	0.113	0.004	0.007	0.047	0.112	0.205	0.359	0.403
		Permafrost	0.269	0.088	0.106	0.126	0.207	0.267	0.328	0.415	0.444
		Autochthonous	0.532	0.110	0.318	0.347	0.456	0.535	0.610	0.709	0.740
		Terrestrial veg	0.061	0.064	0.001	0.002	0.013	0.038	0.088	0.189	0.232
Kolyma	Active layer	0.222	0.181	0.002	0.004	0.052	0.195	0.360	0.544	0.595	
	Permafrost	0.340	0.093	0.148	0.179	0.279	0.346	0.409	0.478	0.502	
	Autochthonous	0.351	0.111	0.152	0.176	0.270	0.345	0.427	0.541	0.574	
	Terrestrial veg	0.087	0.103	0.001	0.001	0.010	0.041	0.137	0.313	0.362	
<b>Summer</b>	FPS	Active layer	0.044	0.052	0.001	0.002	0.010	0.025	0.058	0.151	0.193
		Permafrost	0.116	0.057	0.023	0.034	0.075	0.111	0.152	0.217	0.241
		Autochthonous	0.809	0.090	0.590	0.650	0.763	0.823	0.871	0.926	0.942
		Terrestrial veg	0.031	0.050	0.000	0.001	0.005	0.014	0.035	0.124	0.168
	Headwater	Active layer	0.087	0.101	0.001	0.002	0.015	0.048	0.119	0.298	0.378
		Permafrost	0.088	0.056	0.011	0.017	0.046	0.078	0.119	0.195	0.228
		Autochthonous	0.767	0.137	0.422	0.496	0.694	0.795	0.867	0.942	0.957
		Terrestrial veg	0.058	0.087	0.001	0.001	0.007	0.022	0.067	0.249	0.329
	Wetland	Active layer	0.026	0.032	0.001	0.001	0.006	0.015	0.034	0.088	0.116
		Permafrost	0.034	0.027	0.004	0.005	0.015	0.027	0.047	0.087	0.105
		Autochthonous	0.918	0.058	0.759	0.805	0.895	0.932	0.959	0.981	0.987
		Terrestrial veg	0.021	0.034	0.000	0.001	0.003	0.009	0.025	0.080	0.120
	Tundra	Active layer	0.159	0.149	0.003	0.006	0.038	0.114	0.242	0.456	0.537
		Permafrost	0.215	0.093	0.041	0.064	0.148	0.213	0.278	0.371	0.399
		Autochthonous	0.557	0.141	0.262	0.316	0.463	0.563	0.658	0.782	0.811
		Terrestrial veg	0.070	0.082	0.001	0.002	0.012	0.040	0.098	0.246	0.296
	Forest	Active layer	0.071	0.059	0.004	0.007	0.029	0.055	0.099	0.183	0.222
		Permafrost	0.140	0.056	0.051	0.060	0.099	0.135	0.174	0.239	0.262
		Autochthonous	0.747	0.083	0.559	0.599	0.695	0.757	0.806	0.864	0.880
		Terrestrial veg	0.042	0.042	0.001	0.003	0.012	0.029	0.057	0.128	0.159
Kolyma	Active layer	0.132	0.110	0.003	0.006	0.043	0.105	0.191	0.347	0.405	
	Permafrost	0.216	0.071	0.077	0.098	0.166	0.216	0.264	0.335	0.357	
	Autochthonous	0.589	0.106	0.367	0.403	0.521	0.595	0.664	0.753	0.780	
	Terrestrial veg	0.063	0.067	0.001	0.002	0.013	0.041	0.091	0.198	0.244	

567

568

569 **Data availability**

570 Data will be available within the article or in the Appendix A.

571 **Author contribution**

572 JEV and KHK lead the design of the study with contribution from LB. KHK, LB, DJJ, AD, SD and NZ conducted all the field  
573 work. KHK, LB and DJJ executed all preparatory laboratory work. NH and TIE conducted the AMS analyses, and TT and  
574 PJM analytical laboratory work regarding carbon concentrations and stable isotope analysis. KHK carried out the statistical  
575 analyses. KHK and SBG conducted the spatial analysis. KHK lead the manuscript writing with contribution from all the co-  
576 authors.

577 **Competing interests**

578 The authors declare that they have no conflict of interest.

579 **Acknowledgements**

580 We thank the staff of the Northeast Science Station (NESS) for their support during fieldwork and for providing laboratory  
581 facilities. We want to thank Karel Castro Morales and her team (Friedrich-Schiller University, Jena) and Juri Palmtag  
582 (Northumbria University) for their support in the field. Equally, we want to thank both Suzanne Verdegaal-Warmerdam and  
583 Richard Logtestijn (Vrije Universiteit Amsterdam) for their help with fieldwork preparations. Finally, we thank Niek Speetjens  
584 (Vrije Universiteit Amsterdam) for his advice with the spatial analysis. This study was funded with a starting grant from the  
585 European Research Council to Jorien E. Vonk (THAWSOME #676982), UKRI NERC to Paul J. Mann (CACOON  
586 NE/R012806/1) and NWO Rubicon to Kirsi H. Keskitalo (019.212EN.033). The study of Sergei Davydov, Anna Davydova  
587 and Nikita Zimov was partly carried out within the framework of state assignment number 122020900184-5 of the Pacific  
588 Geographical Institute of RAS.

589 **References**

590 [Adams, H. E., Crump, B. C. and Kling, G. W.: Temperature controls on aquatic bacterial production and community dynamics](#)  
591 [in arctic lakes and streams, \*Environ. Microbiol.\*, 12, 1319–1333, doi:10.1111/j.1462-2920.2010.02176.x, 2010.](#)  
592 [Battin, T.J., Lauerwald, R., Bernhardt, E.S., Bertuzzo, E., Gómez-Gener, L., Hall Jr, R.O., Hotchkiss, E.R., Maavara, T.,](#)  
593 [Pavelisky, T.M., Ran, L., Raymond, P., Rosentreter, J.A. and Regnier, P.: River ecosystem metabolism and carbon](#)  
594 [biogeochemistry in a changing world, \*Nature\*, 613, 449–459, doi:10.1038/s41586-022-05500-8, 2023.](#)

595 Behnke, M.I., Tank, S.E., McClelland, J.W., Holmes, R.M., Haghypour, N., Eglinton, T.I., Raymond, P.A., Suslova, A.,  
596 Zhulidov, A.V., Gurtovaya, T., Zimov, N., Zimov, S., Mutter, E.A., Amos, E. and Spencer, R.G.M.: Aquatic biomass is a  
597 major source to particulate organic matter export in large Arctic rivers. *Proc Natl Acad Sci*, 120,1–9,  
598 doi:<https://doi.org/10.1073/pnas.2209883120>, 2023.

599 Bröder, L., Davydova, A., Davydov, S., Zimov, N., Haghypour, N., Eglinton, T. I. and Vonk, J. E.: Particulate Organic Matter  
600 Dynamics in a Permafrost Headwater Stream and the Kolyma River Mainstem, *J. Geophys. Res. Biogeosciences*, 125, 1–16,  
601 doi:10.1029/2019JG005511, 2020.

602 Buchhorn, M., Smets, B., Bertels, L., De Roo, B., Lesiv, M., Tsendbazar, N.-E., Herold, M. and Fritz, S., Copernicus Global  
603 Land Service: Land Cover 100m: collection 3: epoch 2019, Globe 2020, doi: 10.5281/zenodo.3939050, 2020.

604 Campeau, A., Wallin, M. B., Giesler, R., Löfgren, S., Mörth, C. M., Schiff, S., Venkiteswaran, J. J. and Bishop, K.: Multiple  
605 sources and sinks of dissolved inorganic carbon across Swedish streams, refocusing the lens of stable C isotopes, *Sci. Rep.*, 7,  
606 1–14, doi:10.1038/s41598-017-09049-9, 2017.

607 Collins, C. G., Elmendorf, S. C., Hollister, R. D., Henry, G. H. R., Clark, K., Bjorkman, A. D., Myers-Smith, I. H., Prevéy, J.  
608 S., Ashton, I. W., Assmann, J. J., Alatalo, J. M., Carbognani, M., Chisholm, C., Cooper, E. J., Forrester, C., Jónsdóttir, I. S.,  
609 Klanderud, K., Kopp, C. W., Livensperger, C., Mauritz, M., May, J. L., Molau, U., Oberbauer, S. F., Ogburn, E., Panchen, Z.,  
610 A., Petraglia, A., Post, E., Rixen, C., Rodenhizer, H., Schuur, E. A. G., Semenchuk, P., Smith, J. G., Steltzer, H., Totland, Ø.,  
611 Walker, M. D., Welker, J. M. and Suding, K. N.: Experimental warming differentially affects vegetative and reproductive  
612 phenology of tundra plants, *Nat. Commun.*, 12, 1–12, doi:10.1038/s41467-021-23841-2, 2021.

613 Dean, J. F., Meisel, O. H., Martyn Rosco, M., Marchesini, L. B., Garnett, M. H., Lenderink, H., van Logtestijn, R., Borges, A.  
614 V., Bouillon, S., Lambert, T., Röckmann, T., Maximov, T., Petrov, R., Karsanaev, S., Aerts, R., van Huissteden, J., Vonk, J.  
615 E. and Dolman, A. J.: East Siberian Arctic inland waters emit mostly contemporary carbon, *Nat. Commun.*, 11, 1–10,  
616 doi:10.1038/s41467-020-15511-6, 2020.

617 Denfeld, B. A., Frey, K. E., Sobczak, W. V., Mann, P. J. and Holmes, R. M.: Summer CO<sub>2</sub> evasion from streams and rivers in  
618 the Kolyma River basin, north-east Siberia, *Polar Research* 2013, 32, 19704, doi:10.3402/polar.v32i0.19704, 2013.

619 [Demars, B. O. L., Gíslason, G. M., Ólafsson, J. S., Manson, J. R., Friberg, N., Hood, J. M., Thompson, J. J. D. and Freitag, T.  
620 E.: Impact of warming on CO<sub>2</sub> emissions from streams countered by aquatic photosynthesis. \*Nat. Geosci.\*, 9, 758–761,  
621 doi:10.1038/ngeo2807, 2016.](#)

622 Drake, T. W., Raymond, P. A. and Spencer, R. G. M.: Terrestrial carbon inputs to inland waters: A current synthesis of  
623 estimates and uncertainty, *Limnol. Oceanogr. Lett.*, 3, 132–142, doi:10.1002/lol2.10055, 2018a.

624 Drake, T. W., Guillemette, F. and Hemingway, J. D.: The Ephemeral Signature of Permafrost Carbon in an Arctic Fluvial  
625 Network, *J. Geophys. Res. Biogeosciences*, 123, 1475–1485, doi:10.1029/2017JG004311, 2018b.

626 Fedorov-Davydov, D. G., Davydov, S. P., Davydova, A. I., Ostroymov, V. E., Kholodov, A. L., Sorokovikov, V. A. and  
627 Shmelev, D. G.: The temperature regime of soils in Northern Yakutia, *Earth’s Cryosph.*, 22, 15–24, doi:10.21782/KZ1560-  
628 7496-2018-4, 2018a.

629 Fedorov-Davydov, D. G., Davydov, S. P., Davydova, A. I., Shmelev, D. G., Ostroymov, V. E., Kholodov, A. L. and  
630 Sorokovikov, V. A.: The thermal state of soils in Northern Yakutia, *Earth's Cryosph.*, 22, 52–66, doi:10.21782/KZ1560-7496-  
631 2018-3, 2018b.

632 Guo, L and Macdonald, R.W.: Source and transport of terrigenous organic matter in the upper Yukon River: Evidence from  
633 isotope ( $\delta^{13}\text{C}$ ,  $\Delta^{14}\text{C}$ , and  $\delta^{15}\text{N}$ ) composition of dissolved, colloidal, and particulate phases. *Global Biogeochem. Cycles*, 20,  
634 1-12, doi:10.1029/2005GB002593, 2006.

635 Guo, L., Ping, C. L. and Macdonald, R. W.: Mobilization pathways of organic carbon from permafrost to arctic rivers in a  
636 changing climate, *Geophys. Res. Lett.*, 34, 1–5, doi:10.1029/2007GL030689, 2007.

637 Harrison, W. G. and Cota, G. F.: Primary production in polar waters: relation to nutrient availability, *Polar Res.*, 10, 87–104,  
638 doi:10.3402/polar.v10i1.6730, 1991.

639 Haghypour, N., Ausin, B., Usman, M. O., Ishikawa, N., Wacker, L., Welte, C., Ueda, K. and Eglinton, T. I.: Compound-  
640 Specific Radiocarbon Analysis by Elemental Analyzer-Accelerator Mass Spectrometry: Precision and Limitations *Anal.*  
641 *Chem.*, 91, 2042-2049, doi:10.1021/acsanchem.8b04491, 2019.

642 Holmes, R. M., McClelland, J. W., Peterson, B. J., Tank, S. E., Bulygina, E., Eglinton, T. I., Gordeev, V. V., Gurtovaya, T.  
643 Y., Raymond, P. A., Repeta, D. J., Staples, R., Striegl, R. G., Zhulidov, A. V. and Zimov, S. A.: Seasonal and Annual Fluxes  
644 of Nutrients and Organic Matter from Large Rivers to the Arctic Ocean and Surrounding Seas, *Estuaries and Coasts*, 35, 369–  
645 382, doi:10.1007/s12237-011-9386-6, 2012.

646 Hotchkiss, E.R., Hall, R.O., Sponseller, R.A., Butman, D., Klaminder, J., Laudon, H., Rosvall, M. and Karlsson, J.: Sources  
647 of and processes controlling CO<sub>2</sub> emissions change with the size of streams and rivers. *Nat Geosci*, 8, 696-699,  
648 doi:10.1038/ngeo2507, 2015.

649 Hotchkiss, E. R., Hall, R. O., Baker, M. A., Rosi-Marshall, E. J. and Tank, J. L.: Modeling priming effects on microbial  
650 consumption of dissolved organic carbon in rivers, *J. Geophys. Res. Biogeosciences*, 119, 982–995,  
651 doi:10.1002/2013JG002599, 2014.

652 Hugelius, G., Tarnocai, C., Broll, G., Canadell, J. G., Kuhry, P. and Swanson, D. K.: The northern circumpolar soil carbon  
653 database: Spatially distributed datasets of soil coverage and soil carbon storage in the northern permafrost regions, *Earth Syst.*  
654 *Sci. Data*, 5, 3–13, doi:10.5194/essd-5-3-2013, 2013.

655 Keskitalo, K. H., Bröder, L., Jong, D., Zimov, N., Davydova, A., Davydov, S., Tesi, T., Mann, P. J., Haghypour, N., Eglinton,  
656 T. I. and Vonk, J. E.: Seasonal variability in particulate organic carbon degradation in the Kolyma River, Siberia, *Environ.*  
657 *Res. Lett.*, 17, 034007, doi:https://doi.org/10.1088/1748-9326/ac4f8d, 2022.

658 Keskitalo, K. H., Bröder, L., Tesi, T., Mann, P. J., Jong, D., Bulte Garcia, S., Zimov, N., Davydova, A., Davydov, S.,  
659 Haghypour, N., Eglinton, T. I. and Vonk, J. E.: PANGAEA data set related to this manuscript. DOI to be added, 2023.

660 Levin, I., Kromer, B. and Hammer, S: Atmospheric  $\delta^{14}\text{C}$  trend in Western European background air from 2000 to 2012,  
661 *Tellus, Ser B Chem Phys Meteorol.* 65, 1–7, doi:10.3402/tellusb.v65i0.20092, 2013.

662 Mann, P. J., Davydova, A., Zimov, N., Spencer, R. G. M., Davydov, S., Bulygina, E., Zimov, S. and Holmes, R. M.: Controls  
663 on the composition and lability of dissolved organic matter in Siberia's Kolyma River basin, *J. Geophys. Res. Biogeosciences*,  
664 117, 1–15, doi:10.1029/2011JG001798, 2012.

665 Mann, P. J., Eglinton, T. I., McIntyre, C. P., Zimov, N., Davydova, A., Vonk, J. E., Holmes, R. M. and Spencer, R. G. M.:  
666 Utilization of ancient permafrost carbon in headwaters of Arctic fluvial networks, *Nat. Commun.*, 6, 1–7,  
667 doi:10.1038/ncomms8856, 2015.

668 Mann, P.J., Strauss, J., Palmtag, J., Dowdy, K., Ogneva, O., Fuchs, M., Bedington, M., Torres, R., Polimene, L., Overduin, P.,  
669 Mollenhauer, G., Grosse, G., Rachold, V., Sobczak W.V., Spencer, R.G.M. and Juhls, B.: Degrading permafrost river  
670 catchments and their impact on Arctic Ocean nearshore processes. *Ambio*, 51, 439-455, doi:10.1007/s13280-021-01666-z,  
671 2022.

672 McClelland, J. W., Holmes, R. M., Peterson, B. J., Raymond, P. A., Striegl, R. G., Zhulidov, A. V, Zimov, S. A., Zimov, N.,  
673 Tank, S. E., Spencer, R. G. M., Staples, R., Gurtovaya, T. Y. and Griffin, C. G.: Particulate organic carbon and nitrogen export  
674 from major Arctic rivers, *Global Biogeochem. Cycles*, 30, 629–643, doi:10.1002/ 2015GB005351, 2016.

675 Meredith, M., Sommerkorn, M., Cassotta, S., Derksen, C., Ekaykin, A., Hollowed, A., Kofinas, G., Mackintosh, A.,  
676 Melbourne-Thomas, J Muelbert, M. M. C., Ottersen, G., Pritchard, H. and Schuur, E. A. G.: Polar Regions, in IPCC Special  
677 Report on the Ocean and Cryosphere in a Changing Climate, edited by H.-O. Pörtner, D.-O. Pörtner, D. C. Roberts, V. Masson-  
678 Delmotte, P. Zhai, M. Tignor, J. Petzold, B. Rama, and N. M. Weyer., 2019.

679 [Meyers, P. A.: Preservation of elemental and isotopic source identification of sedimentary organic matter, \*Chem. Geol.\*, 114,](#)  
680 [289–302, doi:10.1016/0009-2541\(94\)90059-0, 1994.](#)

681 Osburn, C. L. and St-Jean, G.: The use of wet chemical oxidation with high-amplification isotope ratio mass spectrometry  
682 (WCO-IRMS) to measure stable isotope values of dissolved organic carbon in seawater *Limnol. Oceanogr. Methods*, 5, 296-  
683 308, doi:104319/lom20075296, 2007.

684 Powers, L. C., Brandes, J. A., Miller, W. L. and Stubbins, A.: Using liquid chromatography-isotope ratio mass spectrometry  
685 to measure the  $\delta^{13}\text{C}$  of dissolved inorganic carbon photochemically produced from dissolved organic carbon, *Limnol.*  
686 *Oceanogr. Methods*, 15, 103–115, doi:10.1002/lom3.10146, 2017.

687 Rantanen M., Karpechko A.Y., Lipponen A., Nordling, K., Hyvärinen, O., Ruosteenoja, K., Vihma, T., and Laaksonen, A.:  
688 The Arctic has warmed nearly four times faster than the globe since 1979, *Commun Earth Environ*, 3, 1-10,  
689 doi:10.1038/s43247-022-00498-3, 2022.

690 Raymond, P.A., Saiers, J.E. and Sobczak, W. V.: Hydrological and biogeochemical controls on watershed dissolved organic  
691 matter transport: Pulse- shunt concept. *Ecology*, 97, 5-16, doi:10.1890/14-1684.1, 2016.

692 R Core Team, R: A language and environment for statistical computing. R Foundation for Statistical Computing, Vienna,  
693 Austria. <https://www.R-project.org/>, 2020.

694 Santoro, M. & Strozzi, T., Circumpolar digital elevation models > 55° N with links to geotiff images DUEPermafrost\_DEM,  
695 doi:10.1594/PANGAEA.779748, 2012.

696 Rogers, J. A., Galy, V., Kellerman, A. M., Chanton, J. P., Zimov, N. and Spencer, R. G. M.: Limited Presence of Permafrost  
697 Dissolved Organic Matter in the Kolyma River, Siberia Revealed by Ramped Oxidation, *J. Geophys. Res. Biogeosciences*,  
698 126, 1–18, doi:10.1029/2020JG005977, 2021.

699 Schuur, E. A. G., McGuire, A. D., Schädel, C., Grosse, G., Harden, J. W., Hayes, D. J., Hugelius, G., Koven, C. D., Kuhry,  
700 P., Lawrence, D. M., Natali, S. M., Olefeldt, D., Romanovsky, V. E., Schaefer, K., Turetsky, M. R., Treat, C. C. and Vonk, J.  
701 E.: Climate change and the permafrost carbon feedback, *Nature*, 520, 171–179, doi:10.1038/nature14338, 2015.

702 Shiklomanov, A.I., R.M. Holmes, J.W. McClelland, S.E. Tank, and R.G.M. Spencer.: Arctic Great Rivers Observatory.  
703 Discharge Dataset, Version 20211118. <https://www.arcticrivers.org/data>, 2021.

704 Siewert, M. B., Hanisch, J., Weiss, N., Kuhry, P., Maximov, T. C. and Hugelius, G.: Comparing carbon storage of Siberian  
705 tundra and taiga permafrost ecosystems at very high spatial resolution, *J. Geophys. Res. Biogeosciences*, 120, 707–723,  
706 doi:10.1002/2015JG002999, 2015.

707 Stadnyk, T. A., Tefs A., Broesky, M., Déry, S. J., Myers, P. G., Ridenour, N. A., Koenig, K., Vonderbank, L., Gustafsson, D.;  
708 Changing freshwater contributions to the Arctic: A 90-year trend analysis (1981–2070), *Elementa: Science of the*  
709 *Anthropocene*, 9, 00098, doi:10.1525/elementa.2020.00098, 2021.

710 Stock, B.C. and Semmens, B.X.: MixSIAR GUI User Manual, :doi: 10.5281/zenodo.1209993, 2016.

711 Stock, B. C. and Semmens, B. X.: Unifying error structures in commonly used biotracer mixing models, *Ecology*, 97, 2562–  
712 2569, doi.org/10.1002/ecy.1517, 2016.

713 Strauss, J., Schirrmeister, L., Grosse, G., Fortier, D., Hugelius, G., Knoblauch, C., Romanovsky, V., Schädel, C., Schneider,  
714 T., Deimling, V., Schuur, E. A. G., Shmelev, D., Ulrich, M. and Veremeeva, A.: Deep Yedoma permafrost : A synthesis of  
715 depositional characteristics and carbon vulnerability, *Earth-Science Rev.*, 172, 75–86, doi:10.1016/j.earscirev.2017.07.007,  
716 2017.

717 Strauss, J., Laboor, S., Schirrmeister, L., Fedorov, A. N., Fortier, D., Froese, D., Fuchs, M., Günther, F., Grigoriev, M., Harden,  
718 J., Hugelius, G., Jongejans, L. L., Kanevskiy, M., Kholodov, A., Kunitsky, V., Kraev, G., Lozhkin, A., Rivkina, E., Shur, Y.,  
719 Siegert, C., Spektor, V., Streletskaia, I., Ulrich, M., Vartanyan, S., Veremeeva, A., Anthony, K. W., Wetterich, S., Zimov, N.  
720 and Grosse, G.: Circum-Arctic Map of the Yedoma Permafrost Domain, *Front. Earth Sci.*, 9, 1–15,  
721 doi:10.3389/feart.2021.758360, 2021.

722 Strauss, J., Laboor, S., Schirrmeister, L., Fedorov, A.N., Fortier, D., Froese, D.G., Fuchs, M., Günther, F., Grigoriev, M.N.,  
723 Harden, J.W., Hugelius, G., Jongejans, L.L., Kanevskiy, M.Z., Kholodov, A.L., Kunitsky, V., Kraev, G., Lozhkin, A.V.,  
724 Rivkina, E., Shur, Y., Siegert, C., Spektor, V., Streletskaia, I., Ulrich, M., Vartanyan, S.L., Veremeeva, A., Walter Anthony,  
725 K.M., Wetterich, S., Zimov, N.S., Grosse, G.; Database of Ice-Rich Yedoma Permafrost Version 2 (IRYP v2). 2022.  
726 doi:<https://doi.org/10.1594/PANGAEA.940078>

727 Striegl, R. G., Dornblaser, M. M., Aiken, G. R., Wickland, K. P. and Raymond, P. A.: Carbon export and cycling by the Yukon,  
728 Tanana, and Porcupine rivers, Alaska, 2001-2005, *Water Resour. Res.*, 43, W02144, doi:10.1029/2006WR005201, 2007.

729 Tank, S. E., Raymond, P. A., Striegl, R. G., McClelland, J. W., Holmes, R. M., Fiske, G. J. and Peterson, B. J.: A land-to-  
730 ocean perspective on the magnitude, source and implication of DIC flux from major Arctic rivers to the Arctic Ocean, *Global*  
731 *Biogeochem. Cycles*, 26, 1–15, doi:10.1029/2011GB004192, 2012.

732 Synal, H. A., Stocker, M. and Suter, M.: MICADAS: A new compact radiocarbon AMS system *Nucl. Instr. and Meth. Phys.*  
733 *Res.*, 25, 7-13, doi:10.1016/j.nimb.200701138, 2007.

734 Turetsky, M. R., Jones, M. C., Walter Anthony, K., Olefeldt, D., Schuur, E. A. G., Koven, C., McGuire, A. D. and Grosse, G.:  
735 Permafrost collapse is accelerating carbon release, *Nature*, 569, 2019.

736 Vonk, J. E., Mann, P. J., Davydov, S., Davydova, A., Spencer, R. G. M., Schade, J., Sobczak, W. V., Zimov, N., Zimov, S.,  
737 Bulygina, E., Eglinton, T. I. and Holmes, R. M.: High biolability of ancient permafrost carbon upon thaw, *Geophys. Res. Lett.*,  
738 40, 2689–2693, doi:10.1002/grl.50348, 2013.

739 Vonk, J. E., Sánchez-García, L., van Dongen, B. E., Alling, V., Kosmach, D., Charkin, A., Semiletov, I. P., Dudarev, O. V.,  
740 Shakhova, N., Roos, P., Eglinton, T. I., Andersson, A. and Gustafsson, Ö.: Activation of old carbon by erosion of coastal and  
741 subsea permafrost in Arctic Siberia, *Nature*, 489, 137–140, doi:10.1038/nature11392, 2012.

742 Waldron, S., Scott, E. M. and Soulsby, C.: Stable isotope analysis reveals lower-order river dissolved inorganic carbon pools  
743 are highly dynamic, *Environ. Sci. Technol.*, 41, 6156–6162, doi:10.1021/es0706089, 2007.

744 Walvoord, M. A. and Kurylyk, B. L.: Hydrologic Impacts of Thawing Permafrost – A Review, *Vadose Zone Journal*, 15, 1–  
745 20, doi:10.2136/vzj2016.01.0010, 2016.

746 Welp, L. R., Randerson, J. T., Finlay, J. C., Davydov, S. P., Zimova, G. M., Davydova, A. I. and Zimov, S. A.: A high-  
747 resolution time series of oxygen isotopes from the Kolyma River: Implications for the seasonal dynamics of discharge and  
748 basin-scale water use, *Geophys. Res. Lett.*, 32, 1–5, doi:10.1029/2005GL022857, 2005.

749 Wang, L. and Liu, H.: An efficient method for identifying and filling surface depressions in digital elevation models for  
750 hydrologic analysis and modelling. *Int. J. Geogr. Inf. Sci.*, 20, 193-213, doi.org/10.1080/13658810500433453, 2006

751 Wild, B., Andersson, A., Bröder, L., Vonk, J., Hugelius, G., McClelland, J. W., Song, W., Raymond, P. A. and Gustafsson,  
752 Ö.: Rivers across the Siberian Arctic unearth the patterns of carbon release from thawing permafrost, *Proc. Natl. Acad. Sci. U.*  
753 *S. A.*, 116, 10280–10285, doi:10.1073/pnas.1811797116, 2019.

754 Winterfeld, M., Goñi, M. A., Just, J., Hefter, J. and Mollenhauer, G.: Characterization of particulate organic matter in the Lena  
755 River delta and adjacent nearshore zone, NE Siberia – Part 2: Lignin-derived phenol compositions, 12, 2261–2283,  
756 doi:10.5194/bg-12-2261-2015, 2015.

757 Winterdahl, M., Wallin, M. B., Karlsen, R. H., Laudon, H., Öquist, M. and Lyon, S. W.: Decoupling of carbon dioxide and  
758 dissolved organic carbon in boreal headwater streams, *J. Geophys. Res. Biogeosciences*, 121, 2630–2651,  
759 doi:10.1002/2016JG003420, 2016.

760 Zimov, S. A., Schuur, E. A. G. and Stuart Chapin, F.: Permafrost and the global carbon budget, *Science*, 312, 1612–1613,  
761 doi:10.1126/science.1128908, 2006.